

National Library  
of CanadaBibliothèque nationale  
du CanadaCANADIAN THESES  
ON MICROFICHETHÈSES CANADIENNES  
SUR MICROFICHENAME OF AUTHOR/NOM DE L'AUTEUR DAVID C. STREDULINSKYTITLE OF THESIS/TITRE DE LA THÈSE Large Deflections of Thin Inextensible  
Elastic RodsUNIVERSITY/UNIVERSITÉ University of AlbertaDEGREE FOR WHICH THESIS WAS PRESENTED/  
GRADE POUR LEQUEL CETTE THÈSE FUT PRÉSENTÉE Master of ScienceYEAR THIS DEGREE CONFERRED/ANNÉE D'OBTENTION DE CE GRADE 1975NAME OF SUPERVISOR/NOM DU DIRECTEUR DE THÈSE M. G. Faulkner

Permission is hereby granted to the NATIONAL LIBRARY OF  
CANADA to microfilm this thesis and to lend or sell copies  
of the film.

The author reserves other publication rights, and neither the  
thesis nor extensive extracts from it may be printed or other-  
wise reproduced without the author's written permission.

L'autorisation est, par la présente, accordée à la BIBLIOTHÈ-  
QUE NATIONALE DU CANADA de microfilmer cette thèse et  
de prêter ou de vendre des exemplaires du film.

L'auteur se réserve les autres droits de publication; ni la  
thèse ni de longs extraits de celle-ci ne doivent être imprimés  
ou autrement reproduits sans l'autorisation écrite de l'auteur.

DATED/DATE April 15 / 1975 SIGNED/SIGNÉ D C StredulinskyPERMANENT ADDRESS/RÉSIDENCE FIXE 30 ~~8910~~ 11255 R.R. 2EdmontonGrande PrairieAlberta

THE UNIVERSITY OF ALBERTA  
LARGE DEFLECTIONS OF THIN INEXTENSIBLE  
ELASTIC RODS

by

(C) DAVID CHARLES STREDULINSKY  
7

A THESIS  
SUBMITTED TO THE FACULTY OF GRADUATE STUDIES AND RESEARCH  
IN PARTIAL FULFILMENT OF THE REQUIREMENTS FOR THE DEGREE  
OF MASTER OF SCIENCE

DEPARTMENT OF MECHANICAL ENGINEERING

EDMONTON, ALBERTA

SPRING, 1975

THE UNIVERSITY OF ALBERTA  
FACULTY OF GRADUATE STUDIES AND RESEARCH

The undersigned certify that they have read, and recommend to the Faculty of Graduate Studies and Research, for acceptance, a thesis entitled Large Deflections of Thin Inextensible Elastic Rods submitted by David Charles Stredulinsky in partial fulfilment of the requirements for the degree of Master of Science.

*Gary Faulkner*.....  
Supervisor

*Donald Quon*.....

*W. Kennedy*.....

*J. B. Macdonald*.....

Date .....April 11, 1975.....

# ABSTRACT

A study is made of thin inextensible elastic rods undergoing large deflections when subject to concentrated and distributed loads.

A general numerical method is developed for solution of the problem of determining the deformed shape of a rod when the loading and boundary conditions are specified. Some specific boundary value problems are solved including the problem of a tapered cantilever bent under its own weight. Experimental verification of the numerical method is given for the problem of a uniform rod pinned at both ends and hanging under its own weight.

The inverse problem of determining the loading of a rod needed to deform it to a specified shape is also considered. Some special analytic solutions are presented and a numerical integration method is used for more general shapes.



## ACKNOWLEDGEMENTS

The author would like to express his appreciation to Dr. M.G. Faulkner for his guidance and supervision. Thanks are due also to Mrs. Elaine Weisenburger for typing this thesis.

# TABLE OF CONTENTS

CHAPTER		PAGE
I	INTRODUCTION	1
II	BASIC CONSIDERATIONS	5
	2.1 Classification of Previously Solved Problems	5
	2.2 Basic Equations	8
	2.3 The Problem of Unknown Deformed Shape	12
	2.4 The Problem of Unknown Free Shape	14
	2.5 The Problem of Unknown Loading	15
III	NUMERICAL SOLUTION OF THE PROBLEM OF UNKNOWN DEFORMED SHAPE	17
	3.1 Basic Numerical Method	17
	3.2 Solution for the Rod Segment	18
	3.3 Equations for the Numerical Method	24
	3.4 Numerical Procedure	33
	3.4.1. Numerical Solution of the Initial Value Problem	33
	3.4.2. Solution of the Boundary Value Problem	36
	3.5 Example Boundary Value Problems	38
	3.5.1. The Elastica Problem	39
	3.5.2. The Cantilever with Uniform Normal Load	47

# TABLE OF CONTENTS (continued)

CHAPTER		PAGE
	3.5.3. The Stiffened Catenary	51
	3.5.4. The Tapered Heavy Cantilever with Concentrated Load	57
IV	SOLUTION OF THE PROBLEM OF UNKNOWN LOADING	63
	4.1 Basic Equations	63
	4.2 Proportional Loading	65
	4.3 Special Solutions	67
	4.3.1. Circular Arc	67
	4.3.2. Linear Variation of Curvature	68
	4.3.3. Normal Loading ( $\mu = 0$ )	71
	4.4 The General Case	72
	4.5 An Example Problem with Shape Specified	74
V	EXPERIMENTAL CONSIDERATIONS	82
	5.1 Experimental Procedure	82
	5.2 Calculations and Results	84
	5.3 Error Analysis	86
VI	CONCLUDING REMARKS	91
	6.1 Summary	91
	6.2 Areas of Further Research	92
	BIBLIOGRAPHY	94
APPENDIX I	GENERAL PROGRAM FOR THE NUMERICAL METHOD OF CHAPTER III	98

TABLE OF CONTENTS (continued)

CHAPTER		PAGE
APPENDIX II	EXPERIMENTAL DATA	109
APPENDIX III	NUMERICAL SOLUTION	111



# LIST OF TABLES

Table	Description	Page
1.	Comparison of the Numerical Method using Different Numbers of Segments to the Analytic Elastica Solution	44
2.	Comparison of the Numerical Method to the Analytic Elastica Solution at Various Points along the Rod	46
3.	Comparison of the Numerical Method with the Analytic Solution for a Cantilever with uniform Normal Load	50
4.	Comparison of the Numerical Method with Lippman et al [16]	62
5.	Percentage Errors in the Numerical and Experimental Solutions	89
6.	Horizontal and Vertical Distances Between Points on Thread	109
7.	Measured Coordinates of Deflected Stiffened Catenary	110
8.	Quantities Calculated using the Numerical Solution for the Stiffened Catenary Problem with $W^* = 1.805$	111

# LIST OF FIGURES

Figure		Page
1.	Offshore Pipeline Installation	2
2.	Free and Deformed Rod Configurations	9
3.	A Small Section of Deformed Rod	9
4.	Section of Rod with Normal and Tangential Loads	9
5.	General Rod Segment	18
6.	Scheme for Assembling Segments	24
7.	Boundary Quantities of Rod	34
8.	The Elastica	40
9.	Cantilever with Normal Load	47
10.	The Stiffened Catenary	52
11.	Position of Global Axis	52
12.	Shapes of Stiffened Catenary with Varying Flexural Stiffness	55
13.	Vertical Deflection and Horizontal Span of Stiffened Catenary	56
14.	The Tapered Cantilever	58
15.	Solution for the Tapered Cantilever with Varying End Load	61
16.	Loading of Rod	64
17.	Polynomial Shapes	75
18.	Nondimensional Normal Loading for Polynomial Shapes	78
19.	Nondimensional Tension for Polynomial Shapes	79

LIST OF FIGURES (continued)

Figure		Page
20.	Nondimensional Shear Force for Polynomial Shapes	80
21.	Nondimensional Moment for Polynomial Shapes	81
22.	Experimental Apparatus	83
23.	Experimental Stiffened Catenary Shapes	85

## CHAPTER I

### INTRODUCTION

In recent years considerable attention has been focused on the production of oil and gas reservoirs through offshore pipelines. The laying of these pipelines in deep water, particularly in the Arctic, can be extremely difficult. One method of installing these pipelines is to lay it continuously from a barge or through a trench in the ice. To avoid buckling or overstressing the pipe during this procedure the radius of curvature of the pipe must be kept above some minimum allowable value. This can be done by supporting the pipe in a bouyant stinger or flexible truss as shown in Figure 1. In designing this supporting structure two types of problems must be solved. In the upper supported region the designer can choose an optimum shape for the pipe. The supporting loads required to give the pipe this shape must then be found. In the lower unsupported region the pipe deforms due to its weight. The loading of the pipe in this region is then known and to check the radius of curvature the deformed shape of the pipe must be determined.

These problems can be solved by treating the pipe as a thin inextensible rod loaded by both distributed and concentrated loads. As in the usual Bernoulli-Euler beam theory the bending moment at any point along the rod is proportional to the curvature at that point. In the small deflection theory this relationship is linearized by

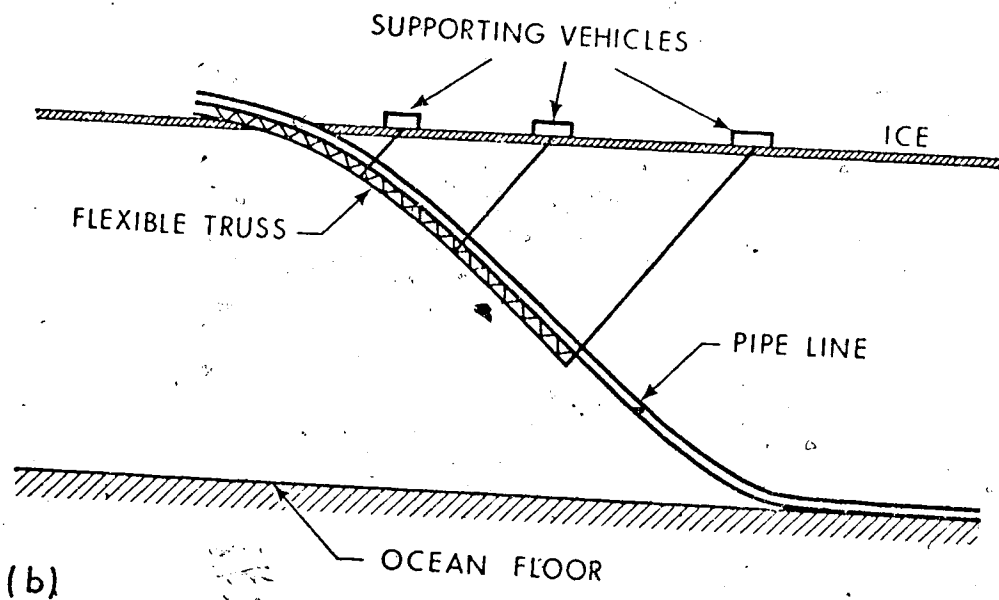
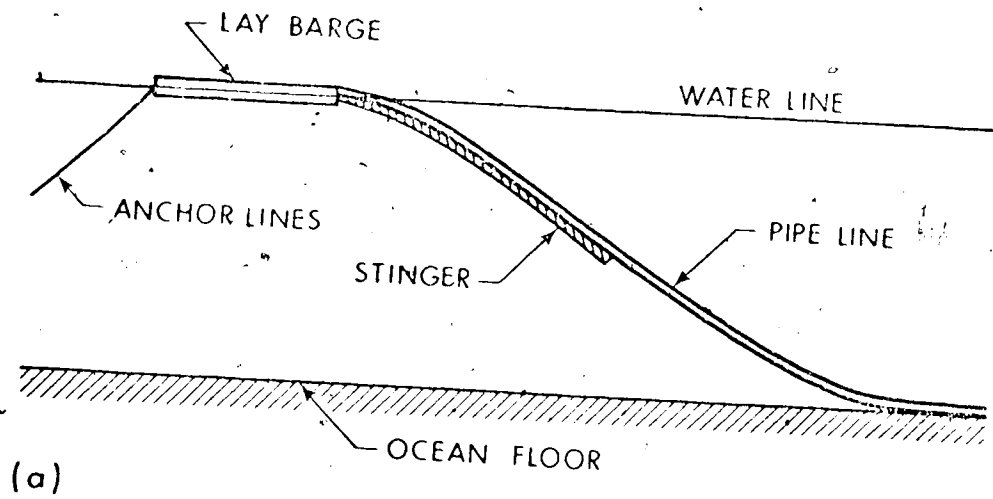


FIGURE 1: Offshore Pipeline Installation

neglecting the square and higher powers of the slope of the rod as small compared to unity. For this problem the square of the slope of the pipeline cannot be neglected and the nonlinear relationship must be used.

The general problem of nonlinear bending of thin rods requires three basic components. These are the free or unloaded shape of the rod, the loading of the rod, and the deformed shape of the rod. The usual problem considered is that in which the free shape and loading of the rod are given. The deformed shape of the rod must then be determined. The inverse problem is that of finding the free shape of the rod when the loading and the deformed shape are specified. A further problem is that in which the free and deformed shapes of the rod are given and the required loading is to be found. The two pipeline problems mentioned previously are special cases of the first and third problems given above where the free shape of the rod is a straight line. The second problem of determining the free shape of the rod is not applicable to the study of initially straight rods.

In Chapter II, the governing differential equations for the three general problems given above are derived. These equations are valid for a rod of varying cross section and subject to nonuniform distributed loading. Chapter III considers the problem of determining the deformed shape of an initially straight rod loaded by distributed and concentrated loads. A general numerical method is presented which can be easily applied to the pipeline problem and to problems

of rods with varying cross section and nonuniform distributed loadings. With this numerical method only a small programable desk computer with limited memory is needed to give accurate solutions. The numerical method is compared to two of the few analytical solutions known for problems of this type. Experimental verification of the numerical method is presented in Chapter V for the case of a thin rod deformed under its own weight when pinned at both ends. The problem of finding the distributed loading necessary to deform an initially straight rod to specified shape is treated in Chapter IV. Some special analytic solutions are given and a numerical integration procedure is used to solve more general problems.

## CHAPTER II

## BASIC CONSIDERATIONS

2.1 Classification of Previously Solved Problems

The problem of nonlinear bending of thin rods has received considerable attention in the past. The usual problem solved is that of determining the deformed shape of the rod when the free shape and loading are specified. The elastic problem of an initially straight rod bent in a plane curve by couples and forces at its end points was first solved by Euler [25]. The problem of an initially straight horizontal cantilever with a vertical concentrated load at its free end was treated approximately by Boyd [4] and Gross and Lehr [12]. Barton [1] and Bisshopp and Drucker [3] later solved this problem in terms of elliptic integrals. Analytical solutions were obtained by Conway [7] and Sato [20] for the case of an initially curved cantilever. Saelman [19] considered the problem of horizontal and vertical loads acting simultaneously at the free end of an initially straight cantilever. The same problem has been solved by Mitchell [17] for an initially curved rod. Frisch-Fay [9] considered the case of a cantilever loaded by several concentrated vertical loads. The problem of a simply supported rod with a central concentrated load has been solved by Conway [6] and Gospodnetic [11].

For problems involving uniformly distributed loads very few analytical solutions have been obtained. Hummel and Morton [14]



presented an approximate solution for the case of a horizontal cantilever subject to a vertical uniformly distributed load. This same case was treated by Bickley [2] and later by Rohde [18] using an approximate series solution. Seames and Conway [22] produced a tabular method using tangential circular arcs which could be used to approximately solve this problem and others, including problems with initially curved rods. Iyengar and Rao [15] used a series solution to solve the problem of a simply supported rod loaded simultaneously by a uniformly distributed load and a central concentrated load. The case of a cantilever subjected to a uniform normal load has been solved analytically by Mitchell [17]. Lippmann, Mahrenholtz and Johnson [16] have used an analog computer to solve various distributed load problems, including that of a cantilever with a varying distributed load and flexural rigidity. The monograph by Frisch-Fay [9] includes mainly solutions of this first type of problem. Reference is made to many of the analytical and numerical solutions mentioned above.

More recently various numerical methods have been used to solve these problems, some giving more accurate results for problems previously considered. A finite difference method has been used by Wang, Lee and Zienkiewicz [29]. Wang [28] has proposed a numerical method which can be used in problems with several concentrated loads. His proposed method for rods with distributed loads is in error as pointed out by Holden [13]. A finite element procedure has been

developed by Tada and Lee [24] for nonlinear bending problems. Schmidt and Da Deppo [21] have used an extension of Rhodes [18] series solution to provide a more accurate solution for the deformed shape of a cantilever with a uniformly distributed load and to provide a solution for the post buckling behavior of a heavy column. The nonlinear bending of a cantilever of variable cross section has been considered by Verma and Krishna Murty [27]. Recently a fourth order Runge-Kutta method has been used by Holden [13] to give accurate solutions for problems with uniformly distributed loads. Yang [30] has used a matrix displacement method to find the deformed shapes of beams and frames with concentrated and distributed loads.

The problem of finding the free shape of a rod necessary to give a specified deformed shape when a known loading is applied has received some attention in the past. Truesdell [26] found the free shape of a cantilever which becomes straight when deformed by a uniformly distributed load. The general solution for the free shape of a cantilever with a specified deformed shape and loading was given by Mitchell [17].

The third type of problem, that in which the free and deformed shapes are specified and the required loading is to be found, has received little attention in the past. This type of problem occurs in the bending of bandsaw blades [10] and in the bending of a pipe to a specified shape [8].

## 2.2 Basic Equations

As in all of the investigations referenced in section 2.1 this work considers the deformation of thin inextensible rods loaded in one plane by static concentrated and distributed loads. It is assumed that the loading and geometry of the rod are such that the rod deforms only in the plane of loading due to bending alone. The rod is assumed to be thin so that the longitudinal strains in the rod remain small. The relative rotations in the rod can still be large and this leads to large deflections of the rod. According to the Bernoulli-Euler law the bending moment  $M$  at any point in the rod is proportional to the change in curvature of the rod. Thus

$$M = EI \left[ \frac{d\theta}{ds} - \frac{d\phi}{ds} \right] \quad (2.1)$$

where  $EI$  is the flexural rigidity of the cross section of the rod and  $\phi(s)$  and  $\theta(s)$  define respectively the free and deformed configurations of the rod as shown in Figure 2.

The equilibrium equations of the rod are given by Frisch-Fay [9] and can be obtained from consideration of a small section of the deformed rod as shown in Figure 3.

$T$ ,  $V$  and  $M$  are the tension, shear force and bending moment respectively. The distributed load per unit length can be resolved into components  $w_x(s)$  and  $w_y(s)$  acting parallel to the  $x$  and  $y$  axis

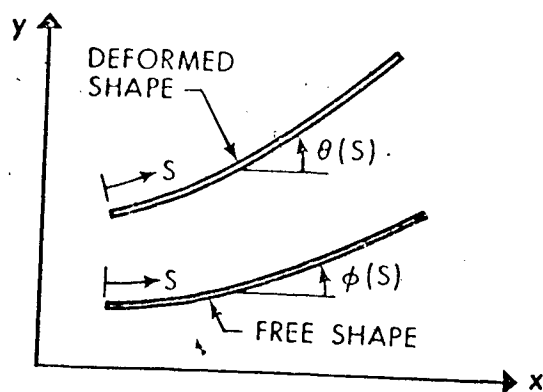


FIGURE 2: Free and Deformed Rod Configurations

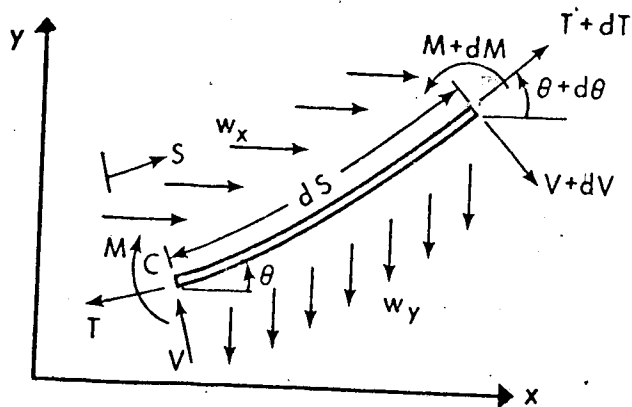


FIGURE 3: A Small Section of Deformed Rod

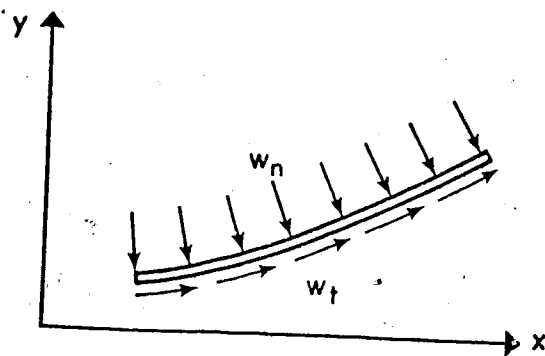


FIGURE 4: Section of Rod with Normal and Tangential Loads

or into components  $w_n(s)$  and  $w_t(s)$  acting normal and tangential to the rod as shown in Figure 4. The static equilibrium of forces resolved in the x and y directions requires

$$\begin{aligned} +\uparrow \Sigma F_y = 0 = & -w_y ds + V \cos \theta - (V + dV) \cos(\theta + d\theta) \\ & - T \sin \theta + (T + dT) \sin(\theta + d\theta) = 0 \end{aligned}$$

After expanding and neglecting second order terms this equation reduces to

$$\frac{d}{ds} (T \sin \theta) - \frac{d}{ds} (V \cos \theta) - w_y = 0 \quad (2.2)$$

Similarly

$$\begin{aligned} +\uparrow \Sigma F_x = 0 = & w_x ds - T \cos \theta + (T + dT) \cos(\theta + d\theta) \\ & + (V + dV) \sin(\theta + d\theta) - V \sin \theta = 0 \end{aligned}$$

which reduces to

$$\frac{d}{ds} (T \cos \theta) + \frac{d}{ds} (V \sin \theta) + w_x = 0 \quad (2.3)$$

In some applications it is more suitable to consider these equations resolved in the normal and tangential directions. This can be done directly by considering the static equilibrium of forces resolved in these directions or by first performing the indicated differentiations

in equations (2.2) and (2.3) and then multiplying equation (2.2) by  $\cos\theta$  and equation (2.3) by  $-\sin\theta$ . Adding the resulting equations gives

$$T \frac{d\theta}{ds} - \frac{dV}{ds} = w_x \sin\theta + w_y \cos\theta = w_n \quad (2.4)$$

Similarly multiplying (2.2) by  $\sin\theta$  and (2.3) by  $\cos\theta$  and adding the two equations gives

$$\frac{dT}{ds} + V \frac{d\theta}{ds} = -w_x \cos\theta + w_y \sin\theta = -w_t \quad (2.5)$$

The moment equilibrium equation requires that

$$\begin{aligned} \sum \mathcal{M}_c = 0 = & M + dM - M - (V + dV) ds + w_x ds \cdot \frac{ds}{2} \sin\theta \\ & - w_y ds \frac{ds}{2} \cos\theta \end{aligned}$$

Neglecting second order quantities gives

$$\frac{dM}{ds} = V. \quad (2.6)$$

The deformed shape of the rod has been expressed in terms of the function  $\theta(s)$ . It is sometimes more convenient to express the shape as  $y = k(x)$ .

These coordinates are related by the following equations

$$\begin{aligned} x &= x_0 + \int_{s_0}^s \cos\theta \, ds \\ y &= y_0 + \int_{s_0}^s \sin\theta \, ds \\ \theta &= \arctan \left( \frac{dy}{dx} \right) \end{aligned} \tag{2.7}$$

$$s = s_0 + \int_{x_0}^x \sqrt{1 + \left( \frac{dy}{dx} \right)^2} \, dx$$

where  $(x_0, y_0)$  are the coordinates of the rod at  $s = s_0$ .

### 2.3 The Problem of Unknown Deformed Shape

In this problem the free shape of the rod  $\phi(s)$  and the distributed loading  $w_x$  and  $w_y$  or  $w_n$  and  $w_t$  and any concentrated loads are specified. The deformed shape of the rod  $\theta(s)$  must then be determined. Integrating equation (2.2) and equation (2.3) gives

$$T \sin\theta - V \cos\theta - \int_0^s w_y \, ds = c_1 \tag{2.8}$$

$$T \cos\theta + V \sin\theta + \int_0^s w_x \, ds = c_2 \tag{2.9}$$

If the boundary conditions  $T = T_0$ ,  $V = V_0$  and  $\theta = \beta$  at  $s = 0$  are

substituted into equations (2.8) and (2.9) then

$$\begin{aligned} c_1 &= T_o \sin\beta - V_o \cos\beta \\ c_2 &= T_o \cos\beta + V_o \sin\beta \end{aligned} \quad (2.10)$$

Multiplying equation (2.8) by  $-\cos\theta$  and equation (2.9) by  $\sin\theta$  and adding gives

$$V + \sin\theta \int_0^s w_x ds + \cos\theta \int_0^s w_y ds = c_2 \sin\theta - c_1 \cos\theta$$

Substituting for  $V$  from equation (2.6) and for  $M$  from equation (2.1) then gives

$$\begin{aligned} \frac{d}{ds} \left[ EI \left( \frac{d\theta}{ds} - \frac{d\phi}{ds} \right) \right] + \sin\theta \int_0^s w_x ds + \cos\theta \int_0^s w_y ds \\ = c_2 \sin\theta - c_1 \cos\theta \end{aligned} \quad (2.11)$$

Equation (2.11) is a second order nonlinear ordinary differential equation for the deformed shape  $\theta(s)$  subject to boundary conditions for a particular problem.

If the normal and tangential loads  $w_n$  and  $w_t$  are specified then equation (2.11) becomes an integral differential equation for  $\theta(s)$  given by



$$\begin{aligned}
& \frac{d}{ds} \left[ EI \left( \frac{d\theta}{ds} - \frac{d\phi}{ds} \right) \right] + \sin\theta \int_0^s (w_t \cos\theta + w_n \sin\theta) ds \\
& + \cos\theta \int_0^s (w_n \cos\theta - w_t \sin\theta) ds \\
& = c_2 \sin\theta - c_1 \cos\theta
\end{aligned} \tag{2.12}$$

A general numerical method is presented in Chapter III for solving this type of problem.

#### 2.4 The Problem of Unknown Free Shape

In this problem the deformed shape  $\theta(s)$  and the loading are specified. The free shape  $\phi(s)$  is to be determined. Rearranging equation (2.11) gives

$$\begin{aligned}
\frac{d}{ds} \left[ EI \frac{d\phi}{ds} \right] &= \frac{d}{ds} \left[ EI \frac{d\theta}{ds} \right] - \sin\theta \int_0^s w_x ds \\
&- \cos\theta \int_0^s w_y ds + c_2 \sin\theta - c_1 \cos\theta
\end{aligned} \tag{2.13}$$

This is a linear second order ordinary differential equation for  $\phi(s)$ . Mitchell [17] gives the general solution of this equation for a cantilever beam. If  $w_n$  and  $w_t$  are specified then equation (2.12) again gives a linear ordinary second order differential equation for  $\phi(s)$ . This problem has been included for completeness and will not be considered further.

## 2.5 The Problem of Unknown Loading

In this problem, the free and deformed shapes of the rod are specified and the required loading must be determined. Substituting for  $V$  in equation (2.4) and (2.5) gives

$$T \frac{d\theta}{ds} - \frac{d^2}{ds^2} \left[ EI \left( \frac{d\theta}{ds} - \frac{d\phi}{ds} \right) \right] - w_n = 0 \quad (2.14)$$

$$\frac{dT}{ds} + \frac{d}{ds} \left[ EI \left( \frac{d\theta}{ds} - \frac{d\phi}{ds} \right) \right] \frac{d\theta}{ds} + w_t = 0 \quad (2.15)$$

These two differential equations involve the unknown functions  $T(s)$ ,  $w_t(s)$  and  $w_n(s)$ . Some additional relation between these functions is required for solution of this problem. For example if the rod is loaded by a normal load  $w_n(s)$  only, then  $w_t = 0$ . Equation (2.15) is then a first order ordinary differential equation which can be solved for the tension  $T(s)$ . Equation (2.14) can then be solved for the required normal load. If the rod is loaded only by a tangential distributed load then equations (2.14) and (2.15) can be solved algebraically for the tension  $T(s)$  and the unknown tangential loading  $w_t$ .

Another more practical case is that of a rod loaded by a known distributed load  $\mathbf{w}$  in the positive  $w_y$  direction (for example the weight of the rod). Proportional normal and tangential loads  $F(s)$  and  $\mu F(s)$  are then applied to the rod to deform it to the required shape. Substituting for this loading in equations (2.14) and (2.15) and eliminating  $F(s)$  from the resulting equations leads to a first order

ordinary differential for  $T(s)$ . The normal load  $F(s)$  can then be obtained from equation (2.14).

Chapter IV considers solutions of this type of problem for the case of an initially straight rod. Analytical solutions are given for special cases and a numerical integration is used for more general shapes.

## CHAPTER III

NUMERICAL SOLUTION OF THE PROBLEM OF  
UNKNOWN DEFORMED SHAPE3.1 Basic Numerical Method

This chapter considers the problem of determining the shape of an initially straight rod loaded by distributed and concentrated loads. The numerical solution presented can be extended to treat initially curved rods.

It was found in section 2.3 that a second order nonlinear differential equation must be solved to obtain the deformed shape of the rod  $\theta(s)$ . The solution of this nonlinear equation can be avoided by considering the rod as a series of short segments. Within each segment only small relative rotations occur while the segment as a whole undergoes large rotations. If the problem is treated as an initial value problem then the overall shape can be built up by solving a linear initial value problem in each segment. The initial conditions used in each segment can be obtained by using geometric and force compatibility conditions at the junction with the previous segment. The actual boundary value problem is solved by considering a series of overall initial value problems which converge to the required boundary conditions.

The use of these segments allows solution of problems involving varying distributed loads and varying flexural rigidity, as well as

problems with several concentrated loads.

### 3.2 Solution for the Rod Segment

Since each segment undergoes only small relative rotations the angle  $\theta$  will be small with respect to some local  $x$  and  $y$  axis as shown in Figure 5.

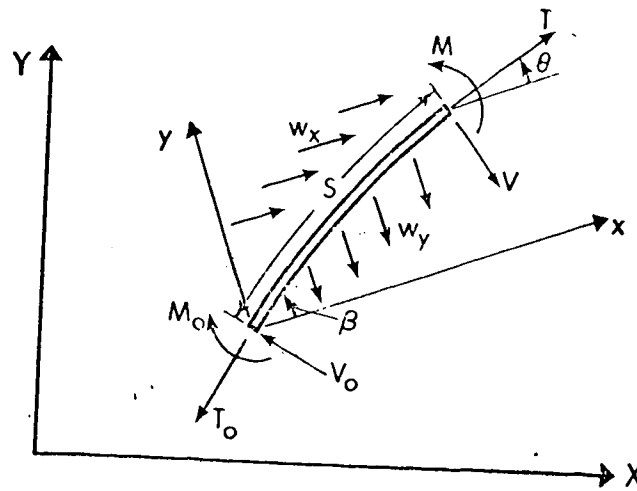


FIGURE 5: General Rod Segment

Neglecting the term  $\theta^2$  as small compared to unity for an initially straight rod equation (2.11) becomes

$$EI \frac{d^2 \theta}{ds^2} + s w_x \theta + s w_y = T_o (\theta - \beta) + V_o \quad (3.1)$$

where  $w_x$  and  $w_y$  are uniform distributed loads acting parallel to the

local  $x$  and  $y$  axis and the flexural rigidity  $EI$  is constant along the element. The constants  $c_1$  and  $c_2$  in equation (2.11) have been evaluated using equation (2.10) for the initial conditions  $T = T_o$ ,  $V = V_o$  and  $\theta = \beta$  at  $s = 0$ .

Equation (3.1) is a linear ordinary differential equation which can be solved for the deformed shape of the segment  $\theta(s)$  subject to the initial conditions  $M = M_o$  and  $\theta = \beta$  at  $s = 0$ .

This equation can be nondimensionalized by multiplying by  $\delta^2$  where  $\delta$  is the length of the segment and then dividing by the flexural rigidity.

This gives

$$\frac{d^2\theta}{d\rho^2} + \left[ \frac{w_x \delta^3}{EI} \rho - \frac{T_o \delta^2}{EI} \right] \theta = \frac{V_o \delta^2}{EI} - \frac{w_y \delta^3}{EI} \rho - \frac{T_o L^2}{EI} \beta \quad (3.2)$$

where  $\rho = \frac{s}{\delta}$ .

Defining the quantities

$$\begin{aligned} \tau_o &= \frac{T_o \delta^2}{EI} & \nu_o &= \frac{V_o \delta^2}{EI} \\ \chi &= \frac{w_x \delta^3}{EI} & \psi &= \frac{w_y \delta^3}{EI} \end{aligned} \quad (3.3)$$

then equation (3.2) can be written as

$$\frac{d^2\theta}{d\rho^2} + [\chi\rho - \tau_0] \theta = v_0 - \tau_0 \beta - \psi\rho \quad (3.4)$$

For an initially straight rod equations (2.1) and (2.6) become

$$M = EI \frac{d\theta}{ds} \quad V = EI \frac{d^2\theta}{ds^2}$$

The nondimensional bending moment and shear force are then given by

$$\mu = \frac{M\delta}{EI} = \frac{d\theta}{d\rho} \quad v = \frac{V\delta^2}{EI} = \frac{d^2\theta}{d\rho^2} \quad (3.5)$$

The solution to the homogeneous part of equation (3.4) can be found in terms of Bessel functions however it is more convenient to use a power series solution.

Assuming

$$\theta = \sum_{k=0}^{\infty} \alpha_k \rho^k \quad (3.6)$$

then the initial conditions  $\theta = \beta$  and

$$\frac{d\theta}{d\rho} = \frac{M_0 \delta}{EI} = \mu_0 \quad \text{at } \rho = 0$$

give

$$\alpha_0 = \beta \quad \alpha_1 = \mu_0 \quad (3.7)$$

Substituting equation (3.6) into the differential equation (3.4) and solving for the coefficient  $\alpha_k$  gives

$$\alpha_2 = v_0/2 \quad \alpha_3 = (\tau_0 \mu_0 - \chi\beta - \psi)/6$$

$$\alpha_k = \frac{\tau_0 \alpha_{k-2} - \chi \alpha_{k-3}}{k(k-1)} \quad k = 4, 5, 6 \dots \quad (3.8)$$

Neglecting the term  $\theta^2$  as small compared to unity gives the local x and y coordinates of the deformed shape from equation (2.7) as

$$x = s$$

$$y = \int_0^s \theta ds$$

where  $x = 0$  and  $y = 0$  at  $s = 0$ . The nondimensional coordinates are then

$$\frac{x}{\delta} = \rho \quad \frac{y}{\delta} = \sum_{k=0}^{\infty} \frac{\alpha_k \rho^{k+1}}{k+1} \quad (3.9)$$

Substituting for  $c_2$  in equation (2.9) from equation (2.10) and applying the small angle approximation gives



$$T = T_o + V_o \beta - V\theta - w_x s$$

where  $w_x$  is constant.

Nondimensionalizing this equation gives

$$\tau = \frac{T\delta^2}{EI} = \tau_o + v_o \beta - v\theta - \chi\rho \quad (3.10)$$

If uniform normal and tangential distributed loads  $w_n$  and  $w_t$  are applied to the segment then equation (2.12) can be used. Applying the small angle approximation to this equation gives

$$\begin{aligned} EI \frac{d^2\theta}{ds^2} + \theta w_t s + \theta w_n \int_0^s \theta ds + w_n s - w_t \int_0^s \theta ds \\ = T_o (\theta - \beta) + V_o \end{aligned}$$

where again the rod is initially straight and the flexural rigidity  $EI$  has been taken as constant in the segment.

Rearranging this equation and defining

$$\bar{\theta}s = \int_0^s \theta ds$$

gives

$$EI \frac{d^2\theta}{ds^2} + w_n (1 + \bar{\theta}) s + w_t (\theta - \bar{\theta}) s = T_o (\theta - \beta) + V_o$$

The term  $\overline{\theta\theta}$  can be neglected compared to unity. This gives

$$\begin{aligned} EI \frac{d^2\theta}{ds^2} + (w_t s - T_o)\theta - w_t \int_0^s \theta ds \\ = V_o - T_o \beta - w_n s \end{aligned} \quad (3.11)$$

Defining

$$\eta = \frac{w_n \delta^3}{EI} \quad \text{and} \quad \xi = \frac{w_t \delta^3}{EI}$$

then equation (3.11) can be nondimensionalized in the same manner as equation (3.2) to give

$$\begin{aligned} \frac{d^2\theta}{d\rho^2} + (\xi\rho - \tau_o)\theta - \xi \int_0^\rho \theta d\rho \\ = v_o - \tau_o \beta - \eta\rho \end{aligned} \quad (3.12)$$

Using the power series solution given by equation (3.6) then  $\alpha_o$  and  $\alpha_1$  are given by equation (3.7).

Substituting this power series into (3.12) yields

$$\begin{aligned} \alpha_2 &= v_o/2 & \alpha_3 &= (\tau_o \mu_o - \eta)/6 \\ \alpha_k &= \frac{\tau_o \alpha_{k-2} - \xi \alpha_{k-3} (1 - 1/k)}{k(k-1)} & k &= 4, 5, 6 \dots \end{aligned} \quad (3.13)$$

Substituting for  $w_x$  and  $c_2$  in equation (2.9) and using the small angle approximation gives

$$T = T_o + V_o \beta - V\theta - w_t s - w_n \int_0^s \theta ds$$

The nondimensional tension is then given by

$$\tau = \tau_o + v_o \beta - v\theta - \xi\rho - \eta y/\delta \quad (3.14)$$

### 3.3 Equations for the Numerical Method

The rod is divided into  $N$  segments each of length  $\delta$ , with the segments numbered from 1 at the starting point to  $N$ . The scheme for assembling the segments is shown in Figure 6

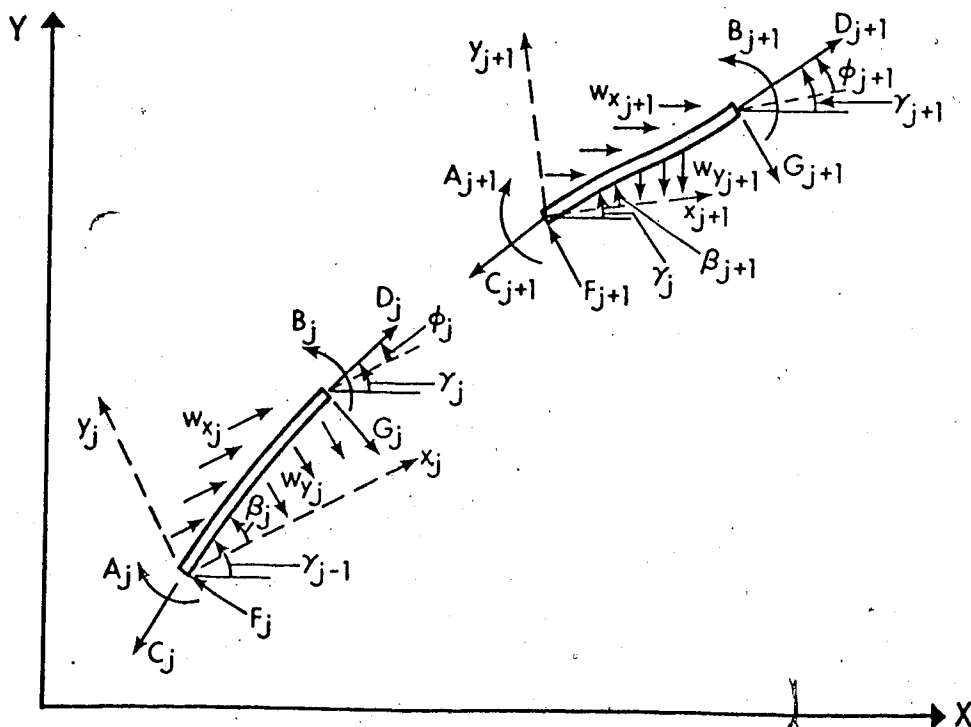


FIGURE 6: Scheme for Assembling Segments

where  $x_j$  and  $y_j$  are the local coordinate axis for the  $j^{\text{th}}$  segment and  $X$  and  $Y$  are the global set of axis.  $\beta_j$  and  $\phi_j$  are respectively the angles from the local  $x_j$  axis to the tangents at the beginning and end of the  $j^{\text{th}}$  segment. The angle  $\gamma_j$  is measured from the global  $X$  axis to the tangent at the end of the  $j^{\text{th}}$  segment.

The bending moments at the beginning and end of the  $j^{\text{th}}$  segment are respectively  $A_j$  and  $B_j$ , the tensions  $C_j$  and  $D_j$  and the shear forces  $F_j$  and  $G_j$  as shown in Figure 6.

Global nondimensional quantities can be defined as

$$\begin{aligned} A_j^* &= \frac{A_j L}{EI^*} & B_j^* &= \frac{B_j L}{EI^*} \\ C_j^* &= \frac{C_j L^2}{EI^*} & D_j^* &= \frac{D_j L^2}{EI^*} \\ F_j^* &= \frac{F_j L^2}{EI^*} & G_j^* &= \frac{G_j L^2}{EI^*} \end{aligned} \quad (3.15)$$

where  $L$  is the length of the rod and  $EI^*$  is a representative flexural rigidity for the rod.

Nondimensional quantities based on the segment length and flexural rigidity of the  $j^{\text{th}}$  segment are

$$\begin{aligned} a_j &= \frac{A_j \delta}{EI_j} & b_j &= \frac{B_j \delta}{EI_j} \\ c_j &= \frac{C_j \delta^2}{EI_j} & d_j &= \frac{D_j \delta^2}{EI_j} \\ f_j &= \frac{F_j \delta^2}{EI_j} & g_j &= \frac{G_j \delta^2}{EI_j} \end{aligned} \quad (3.16)$$

In the numerical method it is necessary to convert from global nondimensional quantities to segment nondimensional quantities at the beginning of the  $j^{\text{th}}$  segment. Using equations (3.15) and (3.16) then

$$a_j = A_j^* / (r_j N) \quad (3.17)$$

$$c_j = C_j^* / (r_j N^2)$$

$$f_j = F_j^* / (r_j N^2)$$

where

$$r_j = \frac{EI_j}{EI^*} \quad (3.18)$$

and  $N$  is the number of segments.

The inverse conversion is used at the end of the  $j^{\text{th}}$  segment given by

$$B_j^* = b_j r_j N$$

$$D_j^* = d_j r_j N^2 \quad (3.19)$$

$$G_j^* = g_j r_j N^2$$

Before the series solution for  $\theta(\rho)$  can be evaluated in the  $j^{\text{th}}$  segment, the angle  $\beta_j$  which determines the position of the  $x_j$  and  $y_j$  axis must be chosen. The simplest choice is to let  $\beta_j$  be zero, then the local axis will be tangent to the beginning of the segment. If the  $x_j$  axis was placed through the end points of the segment, then the angle  $\theta(s)$  measured with respect to this axis intuitively would be smaller at points along the segment than the angle taken with respect to the tangential axis. In deriving the solution for the general segment in section 3.2 the term  $\theta^2$  was neglected as being small compared to unity. It is desirable to make this error term as small as possible in the segment. The average value of  $\theta^2$  in the segment is given by

$$(\theta^2)_{\text{AVE}} = \frac{1}{\rho} \int_0^{\rho} \theta^2 d\rho \quad (3.20)$$

From equations (3.6), (3.7) and (3.8) for the general rod segment

$$\theta = \beta + \mu_0 \rho + \frac{v_0 \rho^2}{2} + \sum_{k=3}^{\infty} \alpha_k \rho^k$$

Approximating  $\theta$  by the first three terms of this series gives

$$\theta = \beta + \mu_0 \rho + \frac{v_0}{2} \rho^2 \quad (3.21)$$

and from equation (3.20) for this linear curvature approximation of the shape

$$(\theta^2)_{\text{AVE}} = \beta^2 + 2\beta\left(\frac{\mu_0}{2} + \frac{v_0}{6}\right) + \frac{\mu_0^2}{3} + \frac{v_0^2}{20} + \frac{\mu_0 v_0}{4}$$

Minimizing this with respect to  $\beta$  gives

$$\beta = -\left(\frac{3\mu_0 + v_0}{6}\right) \quad (3.22)$$

From equation (3.9) the local y-coordinate of the end point of the segment shape given by equation (3.21) is

$$\left(\beta + \frac{\mu_0}{2} + \frac{v_0}{6}\right)$$

which equals zero when  $\beta$  is given by equation (3.22). Thus with this choice of the local x axis passes through the end points of the linear curvature approximation of the deformed shape of the segment.

If only the first two terms of the series are used then this gives a circular arc approximation for the shape of the segment.

Minimizing  $\theta^2_{\text{AVE}}$  gives  $\beta = -\mu_0/2$  which is equivalent to positioning the local axis through the end points of the circular arc approximation of the deformed segment.

If only the first term of the series is used then  $\theta = \beta$  and  $\theta^2_{\text{AVE}}$  is minimized when  $\beta = 0$ . The x-axis is then tangent to the

beginning of the segment. Using equation (3.22) the angle  $\beta_j$  which determines the orientation of the local  $x_j$  and  $y_j$  axis can be chosen as

$$\beta_j = - (3a_j + f_j)/6 \quad (3.23)$$

Evaluating equations (3.5) and (3.6) at the end of the  $j^{\text{th}}$  segment where  $\rho = 1$  gives

$$\begin{aligned} \phi_j &= \sum_{k=0}^{\infty} \alpha_k \\ b_j &= \sum_{k=1}^{\infty} k \alpha_k \\ g_j &= \sum_{k=2}^{\infty} k(k-1) \alpha_k \end{aligned} \quad (3.24)$$

The local coordinates of the end of the segment are

$$\left. \frac{x_j}{\delta} \right|_{\rho=1} = 1 \quad (3.25)$$

and

$$h_j = \left. \frac{y_j}{\delta} \right|_{\rho=1} = \sum_{k=0}^{\infty} \frac{\alpha_k}{k+1} \quad (3.26)$$



If the segment is loaded by constant nondimensional distributed loads  $\chi_j$  and  $\psi_j$  parallel to the  $x_j$  and  $y_j$  axis then from equations (3.7) and (3.8)

$$\begin{aligned}\alpha_0 &= \beta & \alpha_1 &= a_j & \alpha_2 &= f_j/2 \\ \alpha_3 &= (c_j a_j - \chi_j \beta_j - \psi_j)/6\end{aligned}\quad (3.27)$$

$$\alpha_k = (c_j \alpha_{k-2} - \chi_j \alpha_{k-3})/[k(k-1)]$$

$$k = 4, 5, 6 \dots$$

and from equation (3.10)

$$d_j = c_j + f_j \beta_j - g_j \phi_j - \chi_j \quad (3.28)$$

If constant nondimensional distributed loads  $\eta_j$  and  $\xi_j$  act normal and tangential to the  $j^{\text{th}}$  segment then from equations (3.7) and (3.13)

$$\begin{aligned}\alpha_0 &= \beta & \alpha_1 &= a_j & \alpha_2 &= f_j/2 \\ \alpha_3 &= (c_j a_j - \eta_j)/6\end{aligned}\quad (3.29)$$

$$\alpha_k = [c_j \alpha_{k-2} - \xi_j \alpha_{k-3} (1-1/k)]/[k(k-1)]$$

$$k = 4, 5, 6 \dots$$

and from equation (3.14)

$$d_j = c_j - f_j \beta_j - g_j \phi_j - \xi_j - \eta_j h_j \quad (3.30)$$

In some problems both types of constant distributed loads may be applied to the segment. Since both element solutions satisfy linear ordinary differential equations the superposition principle can be used to give the values of  $\alpha_k$  for the combined loading of the  $j^{\text{th}}$  segment.

The angle  $\gamma_j$  at the end of the  $j^{\text{th}}$  segment from Figure 6 is given by

$$\gamma_j = \gamma_{j-1} + \beta_j - \phi_j \quad (3.31)$$

If  $X_j, Y_j$  are the global coordinates of the end of the  $j^{\text{th}}$  segment then from Figure 6.

$$X_j = X_{j-1} + (x_j)|_{\rho=1} \cos(\gamma_{j-1} - \beta_j) - (y_j)|_{\rho=1} \sin(\gamma_{j-1} - \beta_j)$$

$$Y_j = Y_{j-1} + (y_j)|_{\rho=1} \cos(\gamma_{j-1} - \beta_j) + x_j|_{\rho=1} \sin(\gamma_{j-1} - \beta_j)$$

The nondimensional global coordinates of the end of the  $j^{\text{th}}$  segment are then given by

$$\begin{aligned}
 X_j^* &= \frac{X_j}{L} = X_{j-1}^* + \frac{1}{N} [\cos(\gamma_{j-1} - \beta_j) - h_j \sin(\gamma_{j-1} - \beta_j)] \\
 Y_j^* &= \frac{Y_j}{L} = Y_{j-1}^* + \frac{1}{N} [\sin(\gamma_{j-1} - \beta_j) + h_j \cos(\gamma_{j-1} - \beta_j)] \quad (3.32)
 \end{aligned}$$

Given the quantities  $B_j$ ,  $D_j$ ,  $G_j$  at the end of the  $j^{\text{th}}$  segment then if no concentrated forces act on the rod, the forces and bending moment acting at the start of the  $(j+1)^{\text{th}}$  segment are given by

$$A_{j+1} = B_j$$

$$C_{j+1} = D_j$$

$$F_{j+1} = G_j$$

or in nondimensional form

$$A_{j+1}^* = B_j^*$$

$$C_{j+1}^* = D_j^*$$

$$F_{j+1}^* = G_j^*$$

(3.33)

If concentrated forces or couples are applied to the rod then these are assumed to act at the junction of the segments. Equation (3.33) must then be modified to account for these loads.

### 3.4 Numerical Procedure

The usual nonlinear bending problem solved is the two point boundary value problem in which boundary conditions are specified at both ends of the rod. An easier problem to solve is the initial value problem where all boundary conditions are specified at one end of the rod. The numerical procedure for solving this problem is given in subsection 3.4.1. The boundary value problem can be considered as an initial value problem in which some of the initial conditions are not known. If these initial conditions can be found so that the solution to the initial value problem also satisfies the boundary conditions at the end of the rod then this constitutes the solution to the boundary value problem. In subsection 3.4.2 an iterative method is presented which can be used to find these unknown initial conditions and thus obtain the solution to the boundary value problem.

#### 3.4.1. Numerical Solution of the Initial Value Problem

If the bending moment, shear force, tension, global coordinates and slope of the beginning of the rod are known then the solution for the total rod can be built up by solving each segment successively

starting with segment 1. Figure 7 shows a general rod with the six boundary quantities at each end.

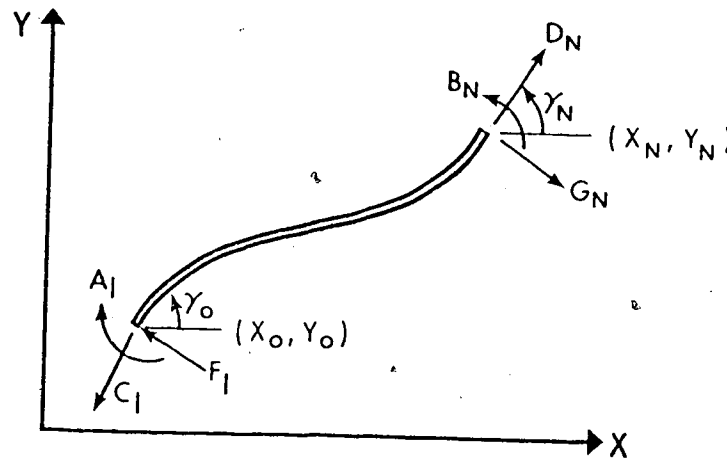


FIGURE 7: Boundary Quantities of Rod

The nondimensional coordinates at the beginning of the rod are given by

$$x_o^* = \frac{x_o}{L} \quad \text{and} \quad y_o^* = \frac{y_o}{L} \quad (3.34)$$

where  $L$  is the length of the rod and the slope is given the angle  $\gamma_o$ . In terms of the notation for the first segment the global nondimensional moment, shear force and tension at the beginning of the rod are  $A_1^*$ ,  $F_1^*$ ,  $C_1^*$ . Given these six quantities then the solution for the first segment can be obtained.

For the  $j^{\text{th}}$  element given the initial quantities  $A_j^*$ ,  $F_j^*$ ,  $C_j^*$ ,  $Y_{j-1}^*$ ,  $X_{j-1}^*$ ,  $Y_{j-1}^*$  and the flexural rigidity ratio  $r_j$  then the following procedure can be used to obtain the quantities at the beginning of the next segment.

1. The segment nondimensional moment  $a_j$ , shear force  $f_j$ , and tension  $c_j$  are calculated from equation (3.17).
2. The angle  $\beta_j$  which determines the local  $x_j$  and  $y_j$  axis is chosen using equation (3.23).
3. The series solution given in equations (3.24) and (3.26) is used to calculate the angle  $\phi_j$  taken with respect to the local  $x_j$  axis, the segment nondimensional moment  $b_j$ , shear force  $g_j$ , and local coordinate  $h_j$  at the end of the  $j^{\text{th}}$  segment. The coefficient  $\alpha_k$  in the series solution are given by equation (3.27) if nondimensional uniform distributed loads  $\chi_j$ ,  $\psi_j$  are applied parallel to the  $x_j$  and  $y_j$  axis. If uniform distributed tangential and normal loads  $\xi_j$  and  $\eta_j$  are applied to the element then the coefficients are given by equation (3.29).
4. The segment nondimensional tension at the end of the  $j^{\text{th}}$  segment  $d_j$  is then given by equation (3.28) if  $\chi_j$  and  $\psi_j$  are applied and by equation (3.30) if loads  $\xi_j$  and  $\eta_j$  are given.
5. The global nondimensional coordinates of the end of the  $j^{\text{th}}$  segment  $X_j^*$ ,  $Y_j^*$  are then calculated from equation (3.32).

6. The angle  $\gamma_j$  defining the slope of the end of the  $j^{\text{th}}$  segment with respect to the global  $X_j$  axis is calculated from equation (3.31).
7. The global nondimensional moment  $B_j^*$ , shear force  $G_j^*$  and tension  $D_j^*$  at the end of the  $j^{\text{th}}$  segment are then obtained from equations (3.19).
8. Equation (3.33) can then be used to calculate the global nondimensional moment  $A_{j+1}^*$ , shear force  $F_{j+1}^*$ , and tension  $D_{j+1}^*$  at the beginning of the  $(j+1)^{\text{th}}$  segment.

The quantities  $A_{j+1}^*$ ,  $F_{j+1}^*$ ,  $C_{j+1}^*$ ,  $\gamma_j$ ,  $X_j^*$ ,  $Y_j^*$  are now known.

The procedure can be repeated successively to obtain the end point quantities for all segments. The nondimensional moment  $B_N^*$ , shear force  $G_N^*$ , tension  $D_N^*$ , coordinates  $X_N^*$  and  $Y_N^*$ , and angle  $\gamma_N$  at the end of the  $N^{\text{th}}$  segment then become the end conditions for the rod as shown in Figure 7.

#### 3.4.2. Solution of the Boundary Value Problem

For the initial value problem six quantities had to be specified at the start of the rod to give a complete solution. In the two point boundary value problem if  $(6-M)$  quantities are specified at the beginning of the rod then  $M$  quantities ( $q_1, q_2, \dots, q_M$ ) must be specified at the end of the rod. Let the specified values of these quantities be  $q_1^*, q_2^*, \dots, q_M^*$ . This means there are  $M$  unknown quantities,

$z_1, z_2, \dots, z_M$  at the beginning of the rod which must be determined.

In vector form these quantities are given by

$$\underline{q} = \begin{bmatrix} q_1 \\ q_2 \\ \vdots \\ q_M \end{bmatrix} \quad \underline{q}^* = \begin{bmatrix} q_1^* \\ q_2^* \\ \vdots \\ q_M^* \end{bmatrix} \quad \underline{z} = \begin{bmatrix} z_1 \\ z_2 \\ \vdots \\ z_M \end{bmatrix} \quad (3.35)$$

The vector  $\underline{q}$  can be treated as a function of  $\underline{z}$  since for given values of  $\underline{z}$  the values of  $\underline{q}$  can be obtained by solving the initial value problem as in section 3.4.1. The boundary value problem can then be solved by finding values of  $\underline{z}$  which satisfy the equation

$$p(\underline{z}) = \underline{q}(\underline{z}) - \underline{q}^* = 0 \quad (3.36)$$

By beginning with the end of the rod which gives the least number of unknown initial conditions then at most equation (3.36) will be by a system of three equations involving three unknowns. By tactful positioning of the global axis, use of overall equilibrium equations and of symmetry of loading and boundary conditions, the number of unknown initial quantities can be reduced to one or two in most problems.

This system of equations can be solved numerically using a variation of Newtons Method. Newtons iteration is given by



$$\underline{z}^{i+1} = \underline{z}^i - \underline{J}^{-1} \underline{p}^i \quad (3.37)$$

where  $\underline{p}^i = \underline{p}(\underline{z}^i)$  and where the  $M \times M$  matrix  $\underline{J}$  has the general term

$$J_{k\ell} = \left. \frac{\partial p_k}{\partial z_\ell} \right|_{\underline{z} = \underline{z}^i}$$

In this problem the above partial differentiation cannot be evaluated. A backward difference formulation can be used instead. The general term of  $\underline{J}$  can then be given as

$$J_{k\ell} = \frac{p_k(\underline{z}^i) - p_k(z_1^i, z_2^i, \dots, z_{\ell-1}^i, z_\ell^{i-1}, z_{\ell+1}^i, \dots, z_M^i)}{z_\ell^i - z_\ell^{i-1}} \quad (3.38)$$

Starting with guesses  $\underline{z}^0$  and  $\underline{z}^1$  then equations (3.37) and (3.38) can be iterated until convergence is obtained. The one dimensional form of this method is usually called the secant method. In this work the  $M$ -dimensional form of this method will be referred to as the  $M$ -dimensional secant method.

### 3.5 Example Boundary Value Problems

This section presents four boundary value problems solved using the numerical method outlined in the previous section. The first problem considered is that of a uniform horizontal cantilever with a horizontal concentrated load applied at the free end. The

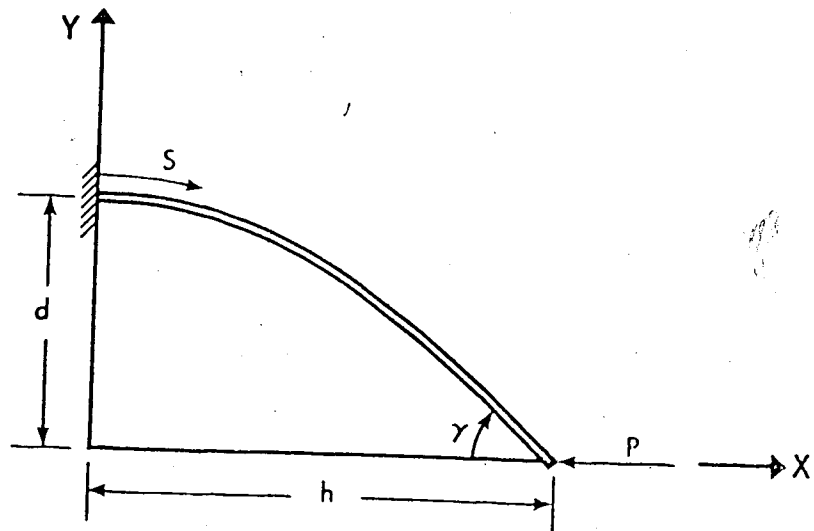
numerical solution with various numbers of segments is compared to the known analytical solution. The problem of a uniform cantilever subject to a uniform normal load is also considered. Again comparison is made to the analytical solution. The third problem is that of a rod of uniform weight per unit length pinned at both ends. No analytical solution of this problem has been found. Experimental verification of the numerical solution of this problem is given in Chapter V. The last problem considered is that of a cantilever of nonuniform flexural stiffness subject to a nonuniform distributed weight loading. The numerical solution is compared to a previous analog computer solution. The same problem with an additional concentrated end load is also considered.

These problems are solved using the general computer program given in Appendix I. Several lines of this program must be specialized to solve a particular problem. Appendix I gives the specialized groups of lines used to solve the above problems.

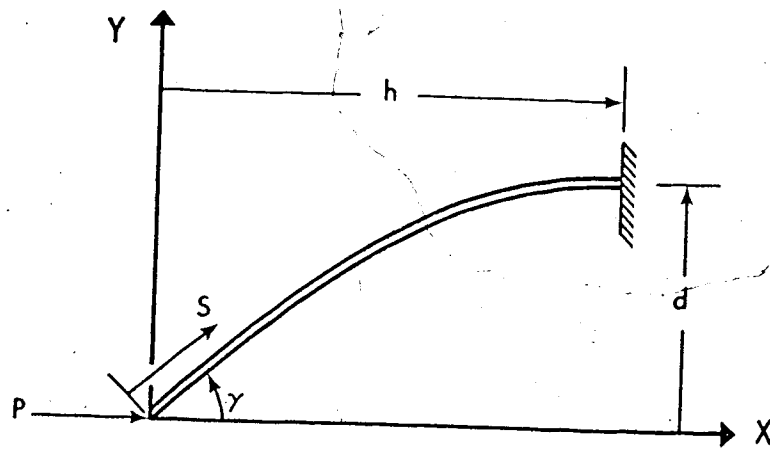
### 3.5.1. The Elastica Problem

This section considers the elastica problem of an initially straight horizontal cantilever loaded by a concentrated horizontal load  $P$  at the free end as shown in Figure 8a. A two point nonlinear boundary value problem must be solved to determine the deformed shape of the rod.

This problem can be solved analytically in terms of elliptic integrals (see Frisch-Fay [9]). With axis located as in Figure 8a, the coordinates of the deformed shape are given by



(a)



(b)

FIGURE 8: The Elastica

$$X^* = X/L = [2E(\phi, p) - F(\phi, p)]/K(p) \quad (3.39)$$

$$Y^* = Y/L = 2p \cos \phi / K(p)$$

where  $L$  is the length of the cantilever,  $p = \sin(\gamma/2)$ ,  $\phi = \text{am}[\rho K(p), p]$  and  $\rho = s/L$ . The nondimensional load is given by

$$P^* = \frac{PL^2}{EI^*} = K^2(p) \quad (3.40)$$

where  $EI^*$  is the flexural rigidity of the rod.  $E(\phi, p)$  and  $F(\phi, p)$  are the incomplete elliptic integrals of the first and second kinds with modulus  $p$  and amplitude  $\phi$ . The complete elliptic integrals of the first and second kinds are  $K(p) = E(\frac{\pi}{2}, p)$  and  $E(p) = E(\frac{\pi}{2}, p)$ .

The lengths  $d$  and  $h$  as shown in Figure 8a are then given from equation (2.39) by

$$\begin{aligned} d^* = \frac{d}{L} &= Y^* \Big|_{\rho=0} = 2p/K(p) \\ h^* = \frac{h}{L} &= X^* \Big|_{\rho=1} = [2E(p) - K(p)]/K(p) \end{aligned} \quad (3.41)$$

The numerical method given in section 3.4 for the solution of boundary value problems can be used in several ways to solve this problem. With the axis positioned as in Figure 8a the  $X$  coordinate and slope are the only quantities specified at the clamped end. At

the free end of the cantilever the X coordinate and slope are not known. By starting at the free end the problem can then be solved using the two dimensional form of the secant method given in section 3.4. If the global coordinate axis are positioned as in Figure 8b then the slope at the free end is the only unknown quantity. The one dimensional secant method can then be used to solve the equation

$$P(Z) = q(Z) - q^* = 0 \quad (3.42)$$

where  $q$  is the slope at the clamped end with specified value  $q^* = 0$  and  $Z = \gamma$  the unknown angle at the free end of the cantilever. In terms of the notation given in Figure 7 for the end conditions of the general rod then the known initial conditions are  $X_0^* = 0$ ,  $Y_0^* = 0$ , the moment  $A_1^* = 0$ , the shear force  $F_1^* = -P^* \sin \gamma$  and tension  $C_1 = -P^* \cos \gamma$ . The unknown initial angle is  $\gamma_0 = \gamma$  and the angle at the clamped end of the rod is  $\gamma_N$ , with specified value  $\gamma_N = 0$ .

The numerical results for this problem were obtained using the general computer program in Appendix I. For the case of a cantilever of uniform cross section the flexural rigidity ratio for the  $j^{\text{th}}$  segment is

$$r_j = \frac{EI_j}{EI^*} = 1.$$

The analytical solution was evaluated using the elliptic integral tables given in reference [23].

In Table 1 the values of  $\gamma$ ,  $d^*$  and  $h^*$  given by these solutions are compared. The subscripts N and A refer respectively to the numerical solution using N segments and to the analytical elliptic integral solution. In the elliptic integral solution the angle  $\gamma$  is first specified and then  $P^*$  is calculated. This value of  $P^*$  is then used in the numerical method.

The program was run with the local segment axis positioned through the end points of the linear curvature approximation to the segment of the rod, through the circular arc approximation, and tangential to the beginning of the segment. Using the linear curvature approximation to position the local axis tended to give the most accurate results. However as the number of segments is increased the differences in the solutions using these three methods become insignificant. Also when the number of segments is doubled the error in the numerical solution is approximately halved. This relationship becomes more exact as the number of segments is increased. If this relationship is satisfied exactly then

$$q^* = 2q_{2N}^* - q_N^* \quad (3.43)$$

where  $q^*$  represents one of the quantities  $\gamma$ ,  $d^*$  or  $h^*$  and the subscripts indicate the number of segments used in the numerical solution. With  $P^* = 4.65056$  then  $h_{80}^* = 0.11908$  and  $h_{160}^* = 0.12111$ , using equation (3.43) gives a better estimate of  $h^*$  as

TABLE 1: Comparison of the Numerical Method  
using Different Numbers of Segments  
to the Analytical Elastica Solution

$$P^* = 2.55406$$

$$\beta_j = -(3a_j + f_j)/5$$

Number of Segments	$\gamma_N$	$d_N^*$	$h_N^*$
1	0.65770	0.41022	0.91233
5	0.55716	0.34392	0.92412
10	0.54064	0.33403	0.92812
20	0.53211	0.32896	0.93026
40	0.52784	0.32642	0.93134
80	0.52572	0.32516	0.93189
160	0.52466	0.32452	0.93216
$2q_{160}^* - q_{80}^*$	0.52360	0.32388	0.93243
Analytical Result	$\gamma_A = 0.52360$	$d_A^* = 0.32390$	$h_A^* = 0.93243$

$$P^* = 4.65056$$

1	2.27013	1.00447	0.01135
5	2.15960	0.81142	0.03114
10	2.13035	0.80572	0.09312
20	2.11305	0.80409	0.10733
40	2.10387	0.80354	0.11507
80	2.09916	0.80334	0.11908
160	2.09679	0.80325	0.12111
$2q_{160}^* - q_{80}^*$	2.09442	0.80316	0.12314
Analytical Result	$\gamma_A = 2.09440$	$d_A^* = 0.80317$	$h_A^* = 0.12316$

$$h^* = 2(.12111) - .11908 = .12314$$

This result is accurate to four significant figures while  $h_{80}^*$  and  $h_{160}^*$  are only correct to two. The values of  $\gamma$ ,  $d^*$  and  $h^*$  given by equation (3.43) with  $N = 80$  are shown in Table 1. This type of convergence was obtained in all problems involving uniform rods with concentrated and uniformly distributed loads.

Table 2 compares the values of the nondimensional  $X$  and  $Y$  coordinates given by the numerical method ( $N = 160$ ) to the analytic elastica solution at five points along the cantilever. For  $P^* = 2.55406$  the rod is approximately parallel to the  $X$  axis. In this case the relative error in the values of  $X^*$  decrease along the rod while the errors in  $Y^*$  increase. For the case of  $P^* = 4.05060$  the rod is approximately parallel to the  $Y$  axis and the errors in  $Y^*$  decrease along the rod while the errors in  $X^*$  increase.



TABLE 2: Comparison of the Numerical Method  
to the Analytic Elastic Solution  
at Various Points along the Rod

$p^* = 2.55406$		$N = 160$	$\beta_j = - (3a_j + f_j)/6$	
$\rho = \frac{s}{L}$	Numerical Method		Analytic Solution	
	$X_{160}^*$	$Y_{160}^*$	$X_A^*$	$Y_A^*$
0.2	0.17394	0.09871	0.17404	0.09853
0.4	0.35256	0.18857	0.35275	0.18822
0.6	0.53888	0.26095	0.53913	0.26046
0.8	0.73306	0.30812	0.73325	0.30753
1.0	0.93216	0.32453	0.93243	0.32390

$p^* = 4.65056$				
0.2	-0.09569	0.17555	-0.09526	0.17579
0.4	-0.16122	0.36396	-0.16030	0.36437
0.6	-0.16026	-0.56281	0.15877	0.56281
0.8	-0.06132	0.73267	-0.05937	0.73281
1.0	0.12111	0.80325	0.12316	0.80317

### 3.5.2. The Cantilever with Uniform Normal Load

This problem is presented to compare the solution using the numerical method to one of the few analytic solutions obtained for rods loaded by distributed loads. The problem of an initially straight cantilever loaded by a uniform normal load per unit length  $P$  has been solved by Mitchell [17].

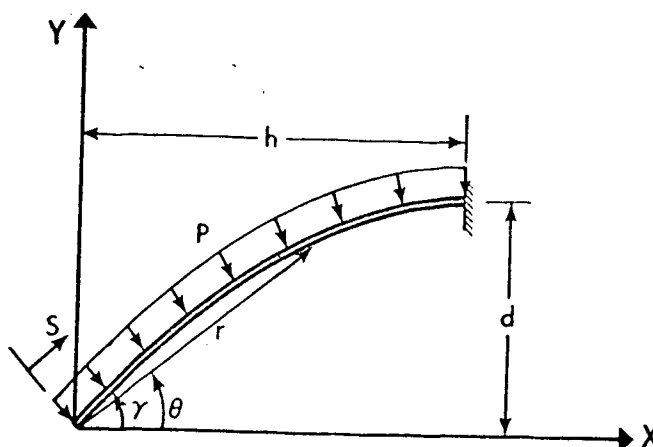


FIGURE 9: Cantilever with Normal Load

In terms of the polar coordinates shown in Figure 9 the deformed shape of the cantilever is given by

$$\theta = \frac{4}{3} \sin^{-1} \left[ \frac{P^*(r^*)^3}{8} \right] - \frac{1}{3} \sin^{-1} \left[ \frac{P^*(r^*)^3}{8} \right] \quad (3.44)$$

where

$$P^* = \frac{PL^3}{EI^*} \quad r^* = \frac{r}{L}$$

and

$$r_L^* = r^* \Big|_{s=L}$$

The nondimensional load  $P^*$  and the radius  $r_L^*$  are related by the equations

$$F(\Omega, k) = \sqrt[4]{3} (P^*)^{1/3} \quad (3.45)$$

where  $F(\Omega, k)$  is the incomplete elliptic integral of the first kind and  $\sin^{-1}(k) = 15^\circ$ . Also

$$\Omega = \cos^{-1} \left[ \frac{1 - (\sqrt{3} + 1)(P^*)^{2/3}(r_L^*)^2/2}{1 + (\sqrt{3} - 1)(P^*)^{2/3}(r_L^*)^2/2} \right] \quad (3.46)$$

These equations can be solved by choosing  $\Omega$ , solving equation (3.45) for  $P^*$  and then using equation (3.46) to determine  $r_L^*$ .

Then

$$\gamma = \theta \Big|_{\rho=0} = \frac{4}{3} \sin^{-1} \left[ \frac{P^*(r_L^*)^3}{8} \right] \quad (3.47)$$

$$h^* = \frac{h}{L} = r_L^* \cos \theta_L$$

$$d^* = \frac{d}{L} = r_L^* \sin \theta_L$$

where

$$\theta_L = \sin^{-1} \frac{P^*(r_L^*)^3}{8}$$

As in the elastica problem this problem can be solved using the one dimensional secant method starting from the free end. The known initial quantities are  $X_0 = 0$ ,  $Y_0 = 0$ ,  $A_1 = 0$ ,  $C_1 = 0$ ,  $F_1 = 0$ . The angle  $\gamma = \gamma_0$  must then be found such that the angle  $\gamma_N$  at the clamped end of the cantilever is given by  $\gamma_N = 0$ .

The nondimensional normal load on the  $j^{\text{th}}$  segment of the rod is

$$\eta_j = \frac{P\delta^3}{EI_j} = P^*/(r_j N^3)$$

where the flexural rigidity ratio  $r_j = 1$  for a cantilever of uniform cross section.

The values of  $\gamma$ ,  $d^*$  and  $h^*$  from the numerical method using the linear curvature approximation to position the segment axis are compared to the analytical results in Table 3. This method tended to give better results than using a circular arc approximation to position the local axis or using tangential segment axis. As in the elastica problem as the number of segments is increased the differences in the results using these three methods become insignificant. Again for large numbers of segments the errors tend to be halved when the number of segments is doubled.

TABLE 3: Comparison of the Numerical Method  
with the Analytical Solution for a  
Cantilever with Uniform Normal Load

$$P^* = 3.29814$$

Number of Segments	$\gamma_N$	$d_N^*$	$h_N^*$
1	0.54969	0.405244	0.92448
2	0.54852	0.397524	0.91181
3	0.54788	0.39567	0.90829
4	0.54749	0.39510	0.90720
5	0.54720	0.39464	0.90676
10	0.54641	0.39385	0.90637
20	0.54590	0.39340	0.90638
40	0.54560	0.39317	0.90647
Analytical Result	$\gamma_A = 0.54530$	$d_A^* = 0.39292$	$h_A^* = 0.90657$

$$P^* = 14.32502$$

1	2.38750	1.11968	-0.32026
3	2.24554	0.82766	-0.09431
5	2.20156	0.81722	-0.07390
10	2.15238	0.81810	-0.04230
20	2.12397	0.82041	-0.02205
40	2.10926	0.82188	-0.01119
80	2.10184	0.82267	-0.00563
160	2.09811	0.82308	-0.00282
Analytical Result	$\gamma_A = 2.09440$	$d_A^* = 0.82350$	$h_A^* = 0.00000$

### 3.5.3. The Stiffened Catenary

The deformed shape of a rod of uniform weight per unit length  $W$  when pinned at both ends has not been determined analytically. Given the coordinates of the ends of the rod and that the bending moment at each end is zero then the three dimensional secant method could be used to determine the three remaining initial conditions. For the symmetric case shown in Figure 10a the vertical component of the reaction at each end of the rod is  $WL$  where  $L$  is the half length of the rod. Using this fact then the problem could be solved using the two dimension secant method.

In Chapter V this problem is treated experimentally with the ends of the rod supported by strings at some angle  $\alpha$  with respect to  $X$  axis as shown in Figure 10b. If the global axis are positioned as in Figure 11 then the solution can be found using a one dimensional secant method starting at the pinned end of the rod.

The known initial conditions are  $X_0^* = 0$ ,  $Y_0^* = 0$ , and the moment  $A_1^* = 0$ . From symmetry the shear force at the mid point of the rod is zero. For equilibrium the vertical component of  $F$  is  $F_y = WL$  and the horizontal component is  $F_x = -WL \cot \alpha$ . The tension and shear force at the beginning of the rod are then

$$C_1 = WL(\sin \gamma + \cot \alpha \cos \gamma)$$

$$F_1 = WL(\cos \alpha - \cot \alpha \sin \gamma)$$

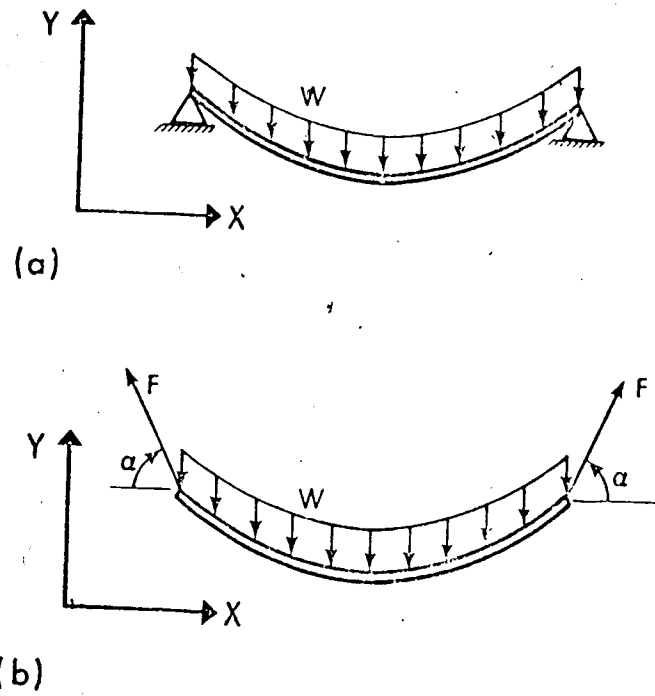


FIGURE 10: The Stiffened Catenary

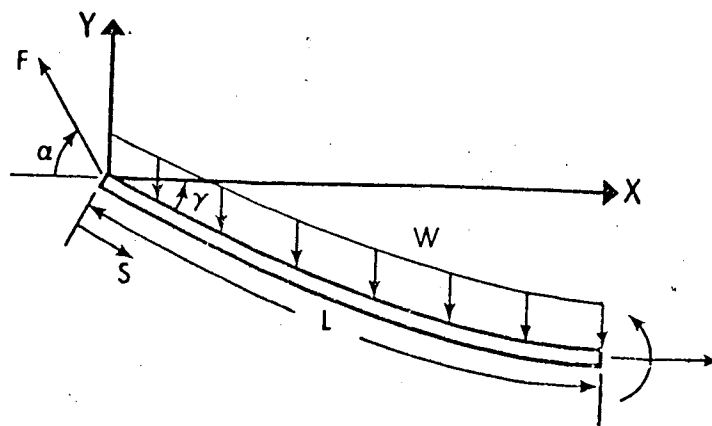


FIGURE 11: Position of Global Axis

In global nondimensional form

$$C_1^* = W^*(\sin \gamma + \operatorname{ctn} \alpha \cos \gamma)$$

$$F_1^* = W^*(\cos \gamma - \operatorname{ctn} \alpha \sin \gamma)$$

where  $W^*$  is the nondimensional weight of half the rod

$$W^* = \frac{WL^3}{EI^*}$$

where the reference flexural rigidity  $EI^*$  is taken as the flexural rigidity of the rod.

The angle  $\gamma_0 = -\gamma$  is the only unknown initial quantity. A one dimensional secant method can be used to find  $\gamma_0$  so that one of the known boundary conditions at the end of the rod, say  $\gamma_N = 0$  is satisfied.

The distributed loads used in the  $j^{\text{th}}$  element are

$$w_x = -W \sin(\gamma_{j-1} - \beta_j)$$

$$w_y = W \cos(\gamma_{j-1} - \beta_j)$$

The nondimensional loads are then



$$x_j = \frac{w}{EI_j} \delta^3 = -W^* \sin(\gamma_{j-1} - \beta_j) / (r_j N^3)$$

$$\psi_j = \frac{w}{EI_j} \delta^3 = W^* \cos(\gamma_{j-1} - \beta_j) / (r_j N^3)$$

For a uniform rod

$$r_j = \frac{EI_j}{EI^*} = 1$$

The numerical results were obtained using the general program in Appendix I specialized for this problem. Figure 12 shows the shape of the rod for various nondimensional weights with  $\alpha = \arctan 2$ . Keeping the angle  $\alpha$  constant and increasing the nondimensional weight  $W^*$  is equivalent to decreasing the stiffness of the rod while keeping the actual weight of the rod and the end reactions constant. As  $W^*$  is increased the shape of the rod approaches the true catenary solution.

Figure 13 can be used to determine the dimensionless vertical deflection  $d^* = d/L$  and the horizontal span  $h^* = h/L$  for rods over the entire range of possible nondimensional weights, and for values of the angle  $\alpha$  ranging from  $\alpha = 0$  to  $\alpha = \pi/2$ . The case of a rod supported only by vertical end reactions occurs when  $\alpha = \pi/2$ . As  $\alpha$  is decreased the horizontal component of the end reaction increases. This horizontal component approaches infinity as  $\alpha$  approaches zero.

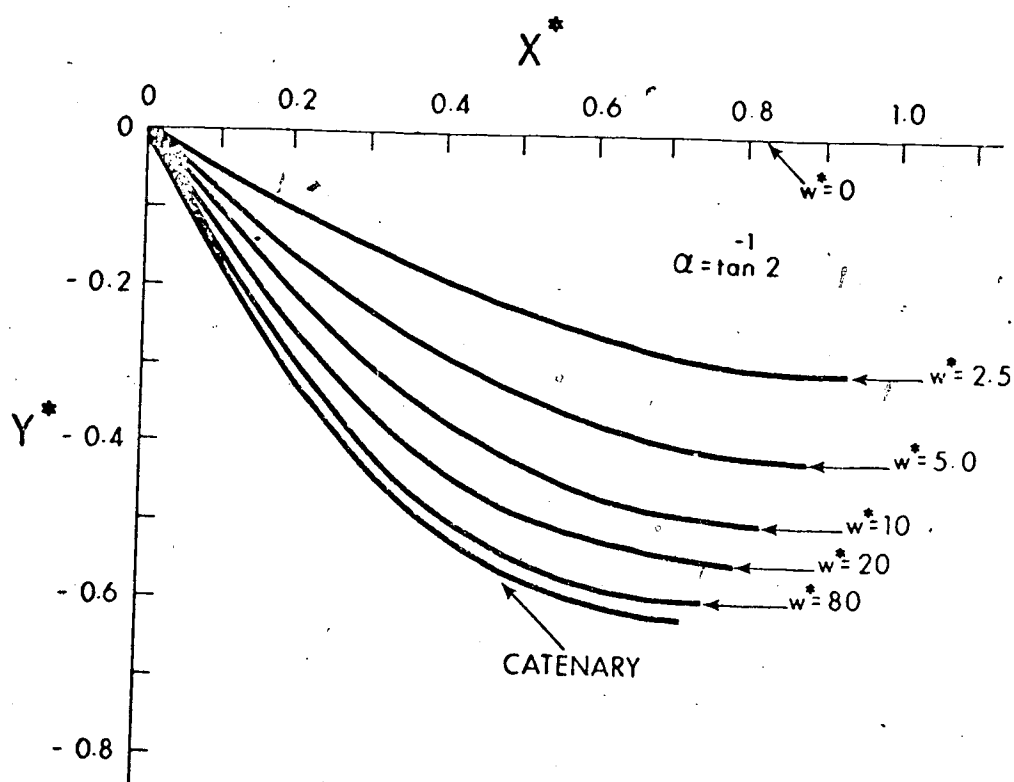


FIGURE 12: Shapes of Stiffened Catenary with Varying Flexural Stiffness

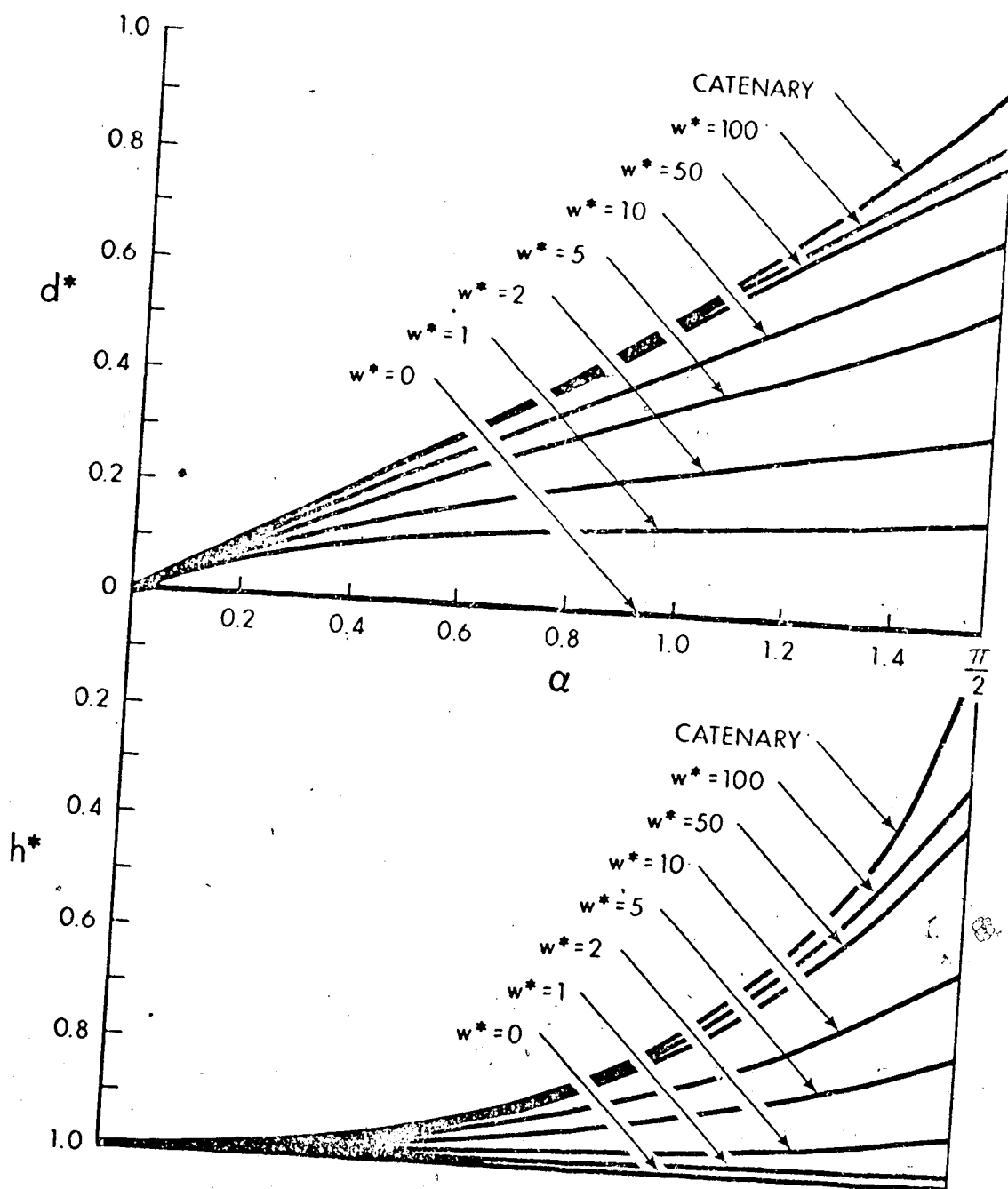


FIGURE 13: Vertical Deflection and Horizontal Span of Stiffened Catenary

### 3.5.4. The Tapered Heavy Cantilever with Concentrated Load

In this problem a trapezoidal strip of uniform density is deformed by its weight and a concentrated load  $P$  at its free end. The load  $P$  will be treated as a follower force acting at a specified angle  $\alpha$  with respect to the cantilever as shown in Figure 14a. It could also be considered as acting at a specified angle to some fixed axis (for example the angle  $\alpha + \gamma$  could be kept constant).

This problem can be solved numerically using a one dimensional secant method starting at the free end. The known initial conditions are  $X_0 = 0$ ,  $Y_0 = 0$ ,  $A_1^* = 0$ ,  $C_1^* = P^* \cos \alpha$  and  $F_1^* = -P^* \sin \alpha$ , where  $P^* = PL^2/EI^*$ . The reference flexural rigidity  $EI^*$  is taken as the flexural rigidity at the base of the cantilever where  $s = L$ .

The top view of the cantilever is shown in Figure 14b. The ratio of the widths is defined as  $t = b_0/b_L$ . If  $t = 0$  then the cantilever is triangular. The special case of a uniform cantilever is given by  $t = 1$ .

The width of the strip at any point is given by

$$b(\rho) = b_L [t + \rho(1-t)] \quad (3.48)$$

where  $\rho = s/L$ .

For a strip of constant thickness the flexural rigidity at any point is proportional to the width of the strip. This gives the flexural rigidity ratio

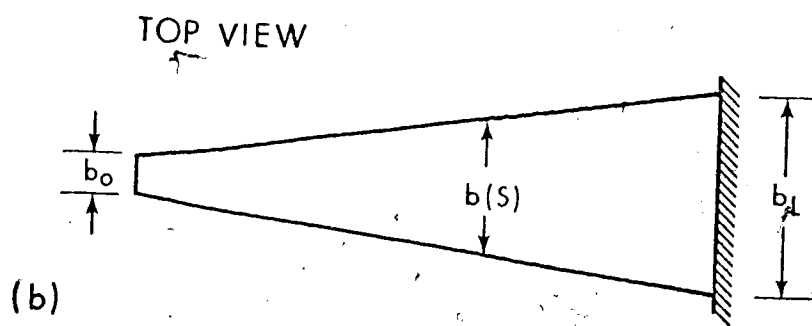
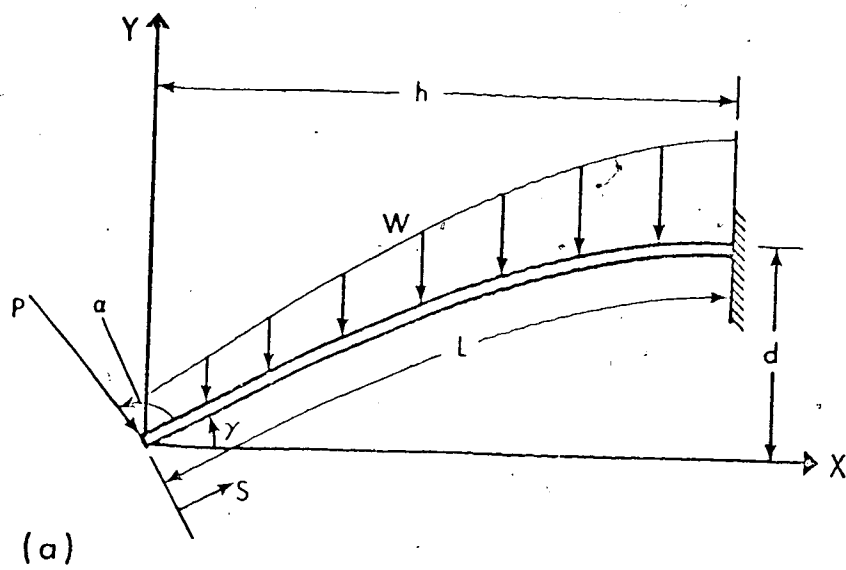


FIGURE 14: The Tapered Cantilever

$$r(\rho) = \frac{EI(\rho)}{EI^*} = t + \rho(1-t) \quad (3.49)$$

The weight per unit length of the strip  $W$  will also be proportional to the width  $b(s)$  giving

$$\frac{W(s)}{W_L} = t + \rho(1-t) \quad (3.50)$$

where  $W_L$  is the weight per unit length of the strip at  $\rho = 1$ .

In the numerical procedure segments with constant flexural rigidity and uniform loads must be used. The shape is approximated by constant width segments with the width taken at the mid point of the segment. Starting at the free end of the strip with segment 1, the mid point of the  $j^{\text{th}}$  segment is given by

$$\rho_j = (j-0.5)/N \quad (3.51)$$

The flexural rigidity ratio for the  $j^{\text{th}}$  element is then

$$r_j = \frac{EI_j}{EI^*} = r(\rho_j) \quad (3.52)$$

The distributed loads in the segment are

$$w_x = -W(\rho_j) \sin(\gamma_{j-1} - \beta_j).$$

$$w_y = W(\rho_j) \cos(\gamma_{j-1} - \beta_j)$$

In nondimensional form after simplification using equations (3.50), (3.51) and (3.52) then

$$\chi_j = \frac{w_x \delta^3}{EI_j} = -W_L^* \sin(\gamma_{j-1} - \beta_j)/N^3$$

$$\psi_j = \frac{w_y \delta^3}{EI_j} = W_L^* \cos(\gamma_{j-1} - \beta_j)/N^3$$

where  $W_L^* = W_L L^3/EI^*$  is the nondimensional weight per unit length at the base of the cantilever.

The general program specialized for this problem as given in Appendix I was run for the special case of a triangular cantilever ( $t = 0$ ) with a variable load  $P$  applied perpendicular to the free end ( $\alpha = \pi/2$ ). The results with  $W_L^* = 10$  are shown in Figure 15. When  $P^*$  is zero the results can be compared to the analog computer solution of Lippman, Mahrenholtz and Johnson [16]. Their results are tabulated for specified values of the angle  $\gamma$ . Given this initial angle  $\gamma_0 = \gamma$  then the loading parameter  $W_L^*$  can be treated as the unknown quantity which must be found using the one dimensional secant method to give a zero slope at the base of the cantilever. Comparison of these results is given in Table 4.

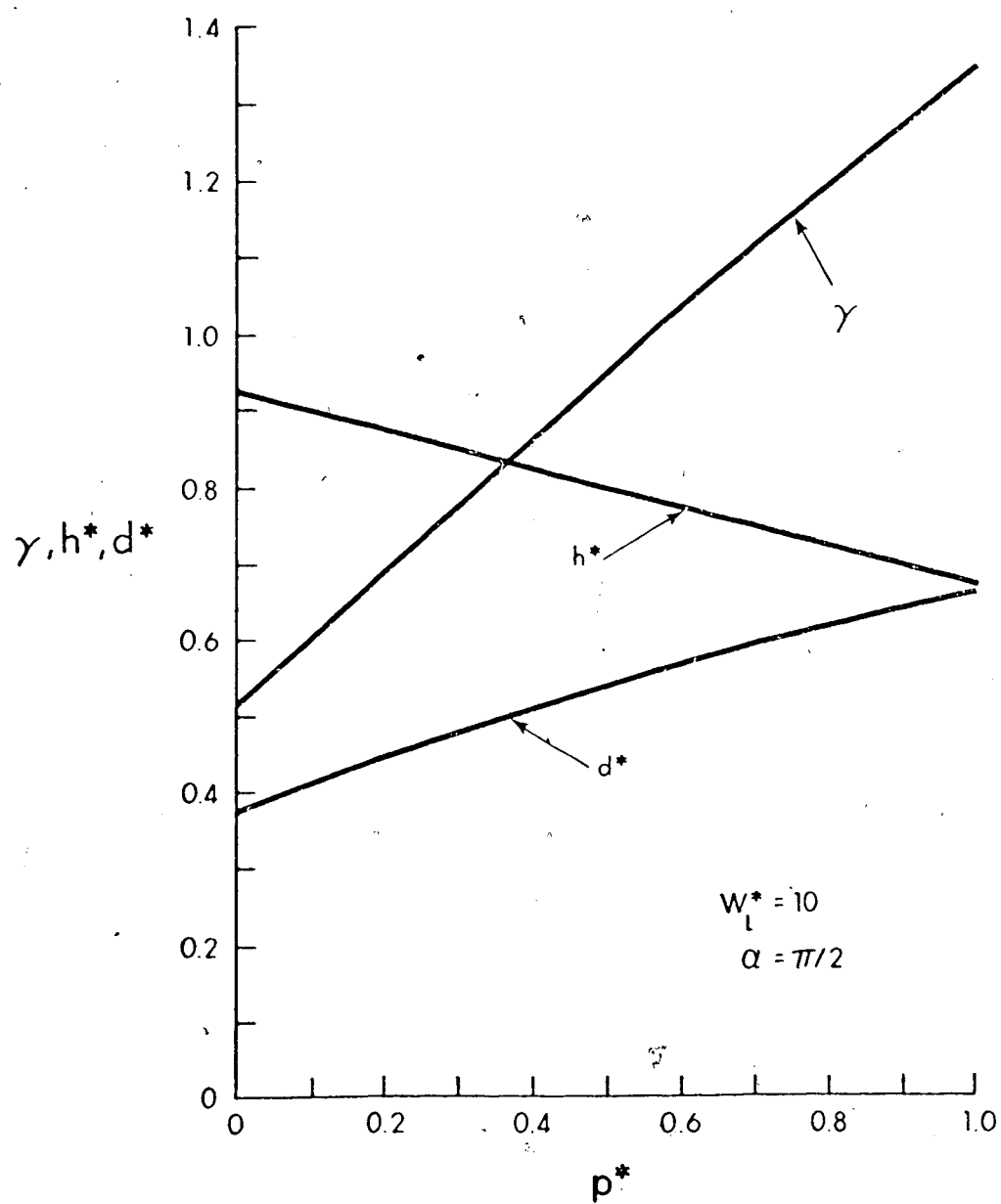


FIGURE 15: Solution for the Tapered Cantilever with Varying End Load



TABLE 4: Comparison of Numerical Method  
with Lippman et al [16]

$\gamma = 10^\circ$

Number of Segments	$h^* = h/L$	$d^* = d/L$	$W^*_L$
10	0.99033	0.12987	3.1081
20	0.99025	0.13033	3.1549
40	0.99023	0.13045	3.1669
80	0.99022	0.13047	3.1700
Reference[16]	0.993	0.129	3.18

$\gamma = 30^\circ$

10	0.91357	0.38018	10.060
20	0.91288	0.38130	10.221
40	0.91271	0.38157	10.266
80	0.91266	0.38163	10.278
Reference[16]	0.899	0.372	10.2

$\gamma = 70^\circ$

10	0.53817	0.78444	39.559
20	0.53563	0.78476	40.354
40	0.53511	0.78468	40.614
80	0.53506	0.78457	40.708
Reference[16]	0.539	0.784	40.7

## CHAPTER IV

## SOLUTION OF THE PROBLEM OF UNKNOWN LOADING

4.1 Basic Equations

The problem of determining the distributed loading necessary to bend a rod to a specified deformed shape was introduced in section 2.5. The special case of an initially straight uniform rod is considered in this chapter. The solutions obtained could be extended to consider initially curved rods.

For many problems the loads are applied normal and tangential to the rod. As well one load which often need be considered is that due to gravity. For these cases the loads  $w_n$  and  $w_t$  shown in Figure 16 are given by

$$w_n = F + W \cos\theta \quad (4.1)$$

$$w_t = G - W \sin\theta \quad (4.2)$$

where  $W$  is the weight per unit length and  $F$  and  $G$  are normal and tangential forces per unit length applied to the rod.

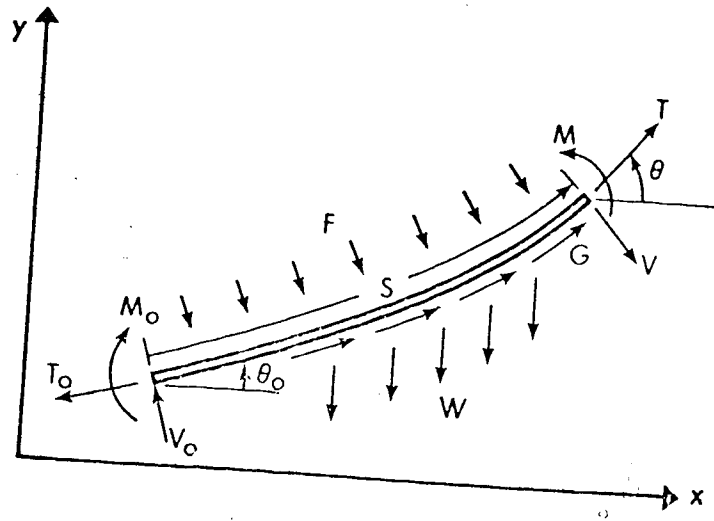


FIGURE 16: Loading of Rod

The equations (2.14) and (2.15) using (4.1) and (4.2) become

$$T \frac{d\theta}{ds} - EI \frac{d^3\theta}{ds^3} = F + W \cos\theta \quad (4.3)$$

$$\frac{dT}{ds} + EI \frac{d^2\theta}{ds^2} \frac{d\theta}{ds} = -G + W \sin\theta \quad (4.4)$$

where the flexural rigidity  $EI$  is constant. Equations (4.3) and (4.4) can be nondimensionalized to give

$$\tau \frac{d\theta}{d\rho} - \frac{d^3\theta}{d\rho^3} = f + w \cos\theta \quad (4.5)$$

$$\frac{d\tau}{d\rho} + \frac{d^2\theta}{2} \frac{d\theta}{d\rho} = -g + \omega \sin\theta \quad (4.6)$$

where the nondimensional quantities used are

$$\begin{aligned} \tau &= \frac{TL^2}{EI} & \omega &= \frac{WL^3}{EI} \\ \rho &= \frac{s}{L} & f &= \frac{FL^3}{EI} & g &= \frac{GL^3}{EI} \end{aligned} \quad (4.7)$$

and in which  $L$  is the length of the rod. The nondimensional moment and shear force are

$$\Omega = \frac{ML}{EI} = \frac{d\theta}{d\rho} \quad \text{and} \quad v = \frac{VL^2}{EI} = \frac{d^2\theta}{d\rho^2} \quad (4.8)$$

In equations (4.5) and (4.6) the deformed shape  $\theta(\rho)$  is known. These equations contain three unknowns  $\tau(\rho)$ ,  $f(\rho)$  and  $g(\rho)$  and therefore some additional relationship between these quantities must be known in order to obtain a solution.

#### 4.2 Proportional Loading

While there are numerous ways in which  $g$  and  $f$  may be related and thereby allow solution of equations (4.5) and (4.6), one possible relationship is

$$g = \mu f \quad (4.9)$$

where  $\mu$  is a constant. This can correspond to the case of frictional resistance such as would occur in a bandsaw blade with impending sliding or during sliding.

Substituting equation (4.9) into equation (4.6) and then eliminating  $f$  from equation (4.5) and (4.6) gives

$$\frac{d\tau}{d\rho} + \mu \frac{d\theta}{d\rho} \tau = -\frac{d^2\theta}{d\rho^2} \frac{d\theta}{d\rho} + \omega \sin\theta + \mu\omega \cos\theta + \mu \frac{d^3\theta}{d\rho^3} \quad (4.10)$$

The solution to this first order linear differential equation is

$$\tau = e^{-\mu\theta} \left[ C + \int e^{\mu\theta} \left( -\frac{d^2\theta}{d\rho^2} \frac{d\theta}{d\rho} + \omega \sin\theta + \mu\omega \cos\theta + \frac{\mu d^3\theta}{d\rho^3} \right) d\rho \right] \quad (4.11)$$

The distributed load  $f$  is then given from equation (4.5) as

$$f = \tau \frac{d\theta}{d\rho} - \frac{d^3\theta}{d\rho^3} - \omega \cos\theta \quad (4.12)$$

The constant  $C$  can be evaluated using

$$\tau = \tau_0 \Big|_{\rho=0} \quad \theta = \theta_0 \Big|_{\rho=0}$$

Equation (4.3) becomes

$$\tau = e^{-\mu\theta} \left[ \tau_0 e^{\mu\theta_0} + \int_0^\rho e^{\mu\theta} \left( -\frac{d^2\theta}{d\rho^2} \frac{d\theta}{d\rho} + \omega \sin\theta + \mu\omega \cos\theta + \frac{\mu d^3\theta}{d\rho^3} \right) d\rho \right] \quad (4.13)$$

The evaluation of equations (4.11) or (4.13) and (4.12) gives the tension in the rod and the normal force distribution. The moment and shear force can be evaluated directly from equation (4.8).

The special case of normal loading alone is given with  $\mu = 0$  in the previous solution. For the case of only tangential loading the normal load  $f$  is zero. From equation (4.5) the tension in the rod is given by

$$\tau = \left( \omega \cos \theta + \frac{d^3 \theta}{d\rho^3} \right) / \frac{d\theta}{d\rho} \quad (4.14)$$

Solving equation (4.6) then gives the tangential load

$$g = \omega \sin \theta - \frac{d^2 \theta}{d\rho^2} \frac{d\theta}{d\rho} - \frac{d\tau}{d\rho} \quad (4.15)$$

### 4.3 Special Solutions

In this section some special solutions of equations (4.12) and (4.13), and equations (4.14) and (4.15) are considered.

#### 4.3.1. Circular Arc

If the rod is bent into the circular arc then

$$\theta = \alpha \rho \quad (4.16)$$

where  $\alpha$  is a constant which corresponds to the nondimensional moment  $\Omega$ .  
The shear force is zero everywhere.

For proportional loading equation (4.13) can be easily integrated to give

$$\tau = \tau_0 e^{-\mu\alpha\rho} + \frac{\omega}{\alpha(1+\mu^2)} [2\mu \sin \alpha\rho + (1-\mu^2)(e^{\mu\alpha\rho} - \cos \alpha\rho)] \quad (4.17)$$

with the corresponding expression for  $f$  from equation (4.12) given by

$$f = \alpha\tau - \omega \cos \alpha\rho \quad (4.18)$$

If only a tangential load is applied to the rod then from equation (4.14)

$$\tau = \frac{\omega}{\alpha} \cos \alpha\rho \quad (4.19)$$

and from equation (4.15) the tangential distributed load is given by

$$g = 2\omega \sin \alpha\rho \quad (4.20)$$

#### 4.3.2. Linear Variation of Curvature

For this case the shape of the rod can be given by

$$\theta = -\frac{\Omega_0}{2} (1 - \rho)^2 + \frac{\Omega_0}{2} + \theta_0 \quad (4.21)$$

where the nondimensional moment at  $\rho = 0$  is  $\Omega_0$  and  $\theta_0$  is the angle.

It has been assumed in equation (4.21) that at  $\rho = 1$  the curvature is zero. The nondimensional shear force in this case is a constant given by

$$v = -\Omega_0$$

For proportional loading equation (3.13) gives

$$\tau = e^{-\mu\theta} \left\{ \tau_0 e^{\mu\theta_0} + \int_0^\rho e^{\mu\theta} [\Omega_0^2 (1-\rho) + \omega \sin\theta + \mu \omega \cos\theta] d\theta \right\} \quad (4.22)$$

where  $\theta$  is given by equation (4.21). This can be reduced to

$$\begin{aligned} \tau = & \left( \tau_0 - \frac{\Omega_0}{\mu} \right) e^{-\mu\Omega_0\rho(2-\rho)/2} + \frac{\Omega_0}{\mu} \\ & + \frac{\omega}{\sqrt{2\Omega_0}} e^{\mu\Omega_0(1-\rho)^2/2} \left[ (\text{sinc} + \mu \text{cosec}) \int_{\Omega_0/2}^{\Omega_0(1-\rho)^2/2} \frac{e^{-\mu u} \cos u}{u^{1/2}} du \right. \\ & \left. + (\mu \omega \text{sinc} + \text{cosec}) \int_{\Omega_0/2}^{\Omega_0(1-\rho)^2/2} \frac{e^{-\mu u} \sin u}{u^{1/2}} du \right] \quad (4.23) \end{aligned}$$

where  $c = \frac{\Omega_0}{2} + \theta_0$ .



The remaining integrals can be evaluated using a power series to give

$$\begin{aligned}
 \tau = & \left( \tau_0 - \frac{\Omega_0}{\mu} \right) e^{-\mu \Omega_0 \rho (2-\rho)/2} + \frac{\Omega_0}{\mu} \\
 & + (1-\rho) \omega e^{\mu \Omega_0 (1-\rho)^2} \left\{ (\text{sinc} + \mu \text{cosec}) \left[ A\left(\frac{\mu \Omega_0 (1-\rho)^2}{2}\right) - A\left(\frac{\Omega_0}{2}\right) \right] \right. \\
 & \left. + (\mu \omega \text{sinc} - \text{cosec}) \left[ B\left(\frac{\mu \Omega_0 (1-\rho)^2}{2}\right) - B\left(\frac{\Omega_0}{2}\right) \right] \right\} \quad (4.24)
 \end{aligned}$$

where

$$A(u) = \sum_{i=0}^{\infty} \sum_{k=0}^{i/2 \text{ or } (i-1)/2} \frac{(-1)^{i-k} \mu^{i-2k} u^i}{2k! (i-2k)! 2^{i+1}}$$

and

$$B(u) = \sum_{i=1}^{\infty} \sum_{k=0}^{\frac{i-1}{2} \text{ or } \frac{i-2}{2}} \frac{(-1)^{i-k-1} \mu^{i-2k-1} u^i}{(2k+1)! (i-2k-1)! (2i+1)}$$

In the summation the upper limit that gives an integer value is used.

Given the nondimensional tension  $\tau$  then normal load  $f$  can be found from equation (4.12). If the load  $\omega$  is zero then the solution is much simpler. From equation (4.23) the tension is given by

$$\tau = \left(\tau_0 - \frac{\Omega_0}{2}\right) e^{-\mu \Omega_0 \rho(2-\rho)/2} + \frac{\Omega_0}{\mu} \quad (4.25)$$

and from equation (3.12) the normal load is then

$$f = \Omega_0(1-\rho) \left[ \left(\tau_0 - \frac{\Omega_0}{2}\right) e^{-\mu \Omega_0 \rho(2-\rho)/2} + \frac{\Omega_0}{\mu} \right] \quad (4.26)$$

#### 4.3.3. Normal Loading ( $\mu = 0$ )

When the external load is normal to the rod equation (4.11) can be integrated in general to give

$$\tau = C + \frac{1}{2} \left(\frac{d\theta}{d\rho}\right)^2 + \omega \int \sin\theta \, d\rho \quad (4.27)$$

for the nondimensional tension. The integral in the last term corresponds, within a constant, to the value of the nondimensional vertical coordinate. The external normal force  $f$  is given by equation (4.12) and the shear force and bending moment can be calculated from equation (4.8).

#### 4.4 The General Case

For the cases in which the shape is such that equations (4.11) or (4.13) cannot be integrated analytically then the integration must be done numerically. Often the specified shape is given in terms of the cartesian coordinates instead of the function  $\theta(s)$ .

When the shape is given as  $y = k(x)$  a Simpson's rule integration procedure is used to first determine the length of the rod  $L$  from the equation

$$L = \int_0^d [1 + \left(\frac{dy}{dx}\right)^2]^{1/2} dx \quad (4.28)$$

where  $d$  is the horizontal distance between the ends of the required shape. Once the length is known the shape function is put into the form

$$\lambda = \frac{x}{L} = \tilde{k}(\xi), \quad \xi = \frac{x}{L} \quad (4.29)$$

From equation (2.7) in terms of the nondimensional coordinates

$$\theta = \arctan \left( \frac{d\lambda}{d\xi} \right)$$

and

(4.30)

$$\frac{d\xi}{d\rho} = [1 + \left(\frac{d\lambda}{d\xi}\right)^2]^{-1/2}$$

Equations (4.30) can be used to obtain the following derivatives.

$$\begin{aligned}
 \frac{d\theta}{d\rho} &= \frac{d^2\lambda}{d\xi^2} [1 + (\frac{d\lambda}{d\xi})^2]^{-3/2} \\
 \frac{d^2\theta}{d\rho^2} &= \frac{d^3\lambda}{d\xi^3} [1 + (\frac{d\lambda}{d\xi})^2]^{-2} - 3 \frac{d\lambda}{d\xi} (\frac{d^2\lambda}{d\xi^2}) [1 + (\frac{d\lambda}{d\xi})^2]^{-3} \\
 \frac{d^3\theta}{d\rho^3} &= \frac{d^4\lambda}{d\xi^4} [1 + (\frac{d\lambda}{d\xi})^2]^{-5/2} - 10 (\frac{d^3\lambda}{d\xi^3}) (\frac{d^2\lambda}{d\xi^2}) \frac{d\lambda}{d\xi} [1 + (\frac{d\lambda}{d\xi})^2]^{-7/2} \\
 &\quad - 3 (\frac{d^2\lambda}{d\xi^2})^3 [1 + (\frac{d\lambda}{d\xi})^2]^{-7/2} + 18 (\frac{d^2\lambda}{d\xi^2})^2 (\frac{d\lambda}{d\xi})^2 [1 + (\frac{d\lambda}{d\xi})^2]^{-9/2}
 \end{aligned}
 \tag{4.31}$$

These expressions can be substituted in equation (4.13) to give an expression of the following form for the tension  $\tau$  as a function of  $\xi$

$$\tau(\xi) = e^{-\mu\theta(\xi)} \left[ 1 + \int_0^\xi R(\xi) d\xi \right]
 \tag{4.32}$$

From equation (4.30) the coordinate  $\rho$  is given

$$\rho(\xi) = \int_0^\xi [1 + (\frac{d\lambda}{d\xi})^2]^{1/2} d\xi
 \tag{4.33}$$

where  $\rho = 0$  at  $\xi = 0$ .

The integrals in equation (4.32) and (4.33) can be evaluated numerically using a Simpson rule integration procedure.

The normal load  $f(\xi)$  can then be evaluated by substituting equations (4.30) and (4.31) into equation (4.12). Similarly the moment  $\Omega(\xi)$  and shear force  $v(\xi)$  can be evaluated by substituting for  $\frac{d\theta}{d\rho}$  and  $\frac{d^2\theta}{d\rho^2}$  in equation (4.8) from equation (4.31).

#### 4.5 An Example Problem with Shape Specified

As an example consider the family of shapes shown in Figure 17. The shape is given by a seventh order polynomial

$$y = \sum_{i=0}^7 a_i x^i \quad (4.34)$$

which satisfies the conditions

$$y(0) = y'(0) = y''(0) = 0$$

$$y(d) = h \quad y'(d) = y''(d) = 0 \quad (4.35)$$

$$y\left(\frac{d}{2}\right) = \frac{h}{2} \quad y'\left(\frac{d}{2}\right) = C$$

The conditions in (4.35) correspond to a rod that has zero slope and moment on the two ends. Also the rod has a change in elevation of  $h$  for a horizontal distance  $d$ . The second last condition ensures

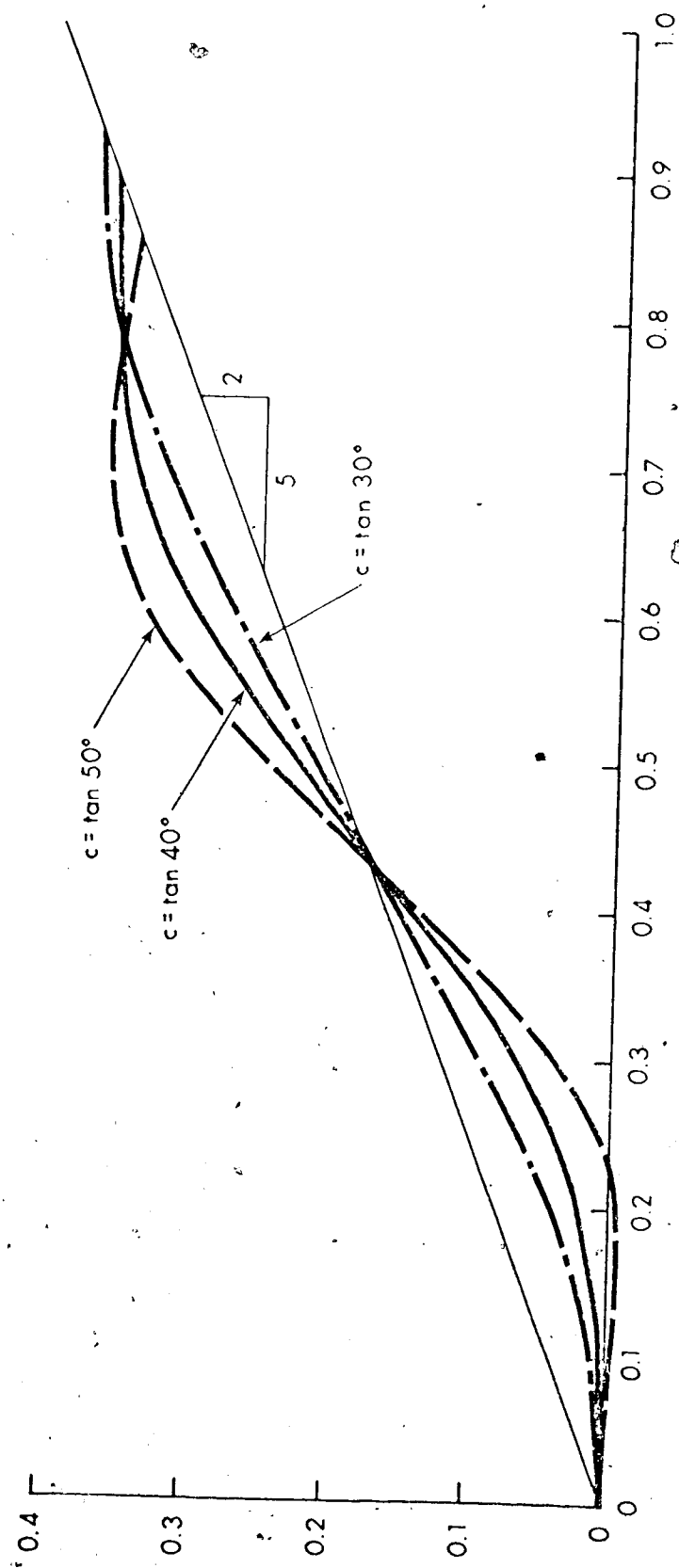


FIGURE 17: Polynomial Shapes

symmetry about the mid point while the last is used to give a family of shapes.

Using these conditions the coefficients in (4.34) are

$$a_0 = a_1 = a_2 = 0$$

$$\begin{bmatrix} a_3 d^2 \\ a_4 d^3 \\ a_5 d^4 \\ a_6 d^5 \\ a_7 d^7 \end{bmatrix} = \begin{bmatrix} 70 & -32 \\ -315 & 160 \\ 546 & -288 \\ -420 & 224 \\ 120 & -64 \end{bmatrix} \begin{bmatrix} h/d \\ C \end{bmatrix} \quad (4.36)$$

Given  $C$ ,  $h$  and  $d$  the length of the rod  $L$  can be found from equation (4.28).

The nondimensional coordinates of the shape are then given by

$$\lambda = \sum_{i=0}^7 b_i \xi^i \quad (4.37)$$

where  $b_i = a_i L^{i-1}$   $i = 0, 1, 2, \dots, 7$ .

Figure 17 shows the shapes of the rod in nondimensional form with  $h/d = 0.4$  for three values of  $C$ .

The forces required to maintain these shapes can be calculated using the procedure of section 4.4. For this problem the normal load is positive and negative in different regions of the rod. To keep the frictional force applied in one direction along the rod  $\mu$  was taken as positive in the region where the normal force was positive and as negative where the normal force was negative. Figure 18 shows the normal forces required for the case of  $\omega = 100$  and  $\mu = 0.1$ . The initial tension at  $\rho = 0$  was taken as  $\tau_0 = 10$ . The tension in the rod for three values of  $C$  is shown in Figure 19. The shear force and bending moments along the rod are shown respectively in Figures 20 and 21.



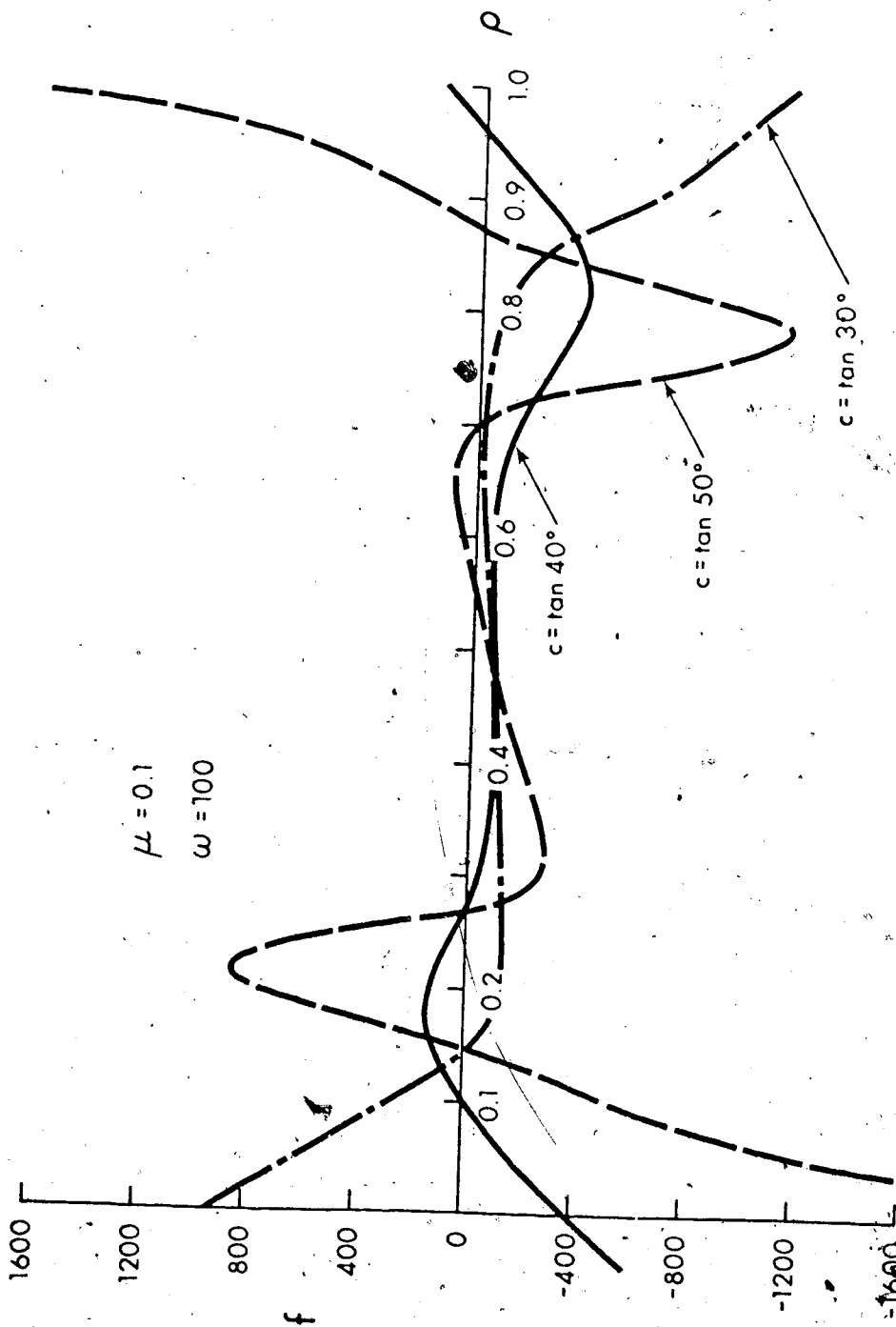


FIGURE 18: Nondimensional Normal Loading for Polynomial Shapes

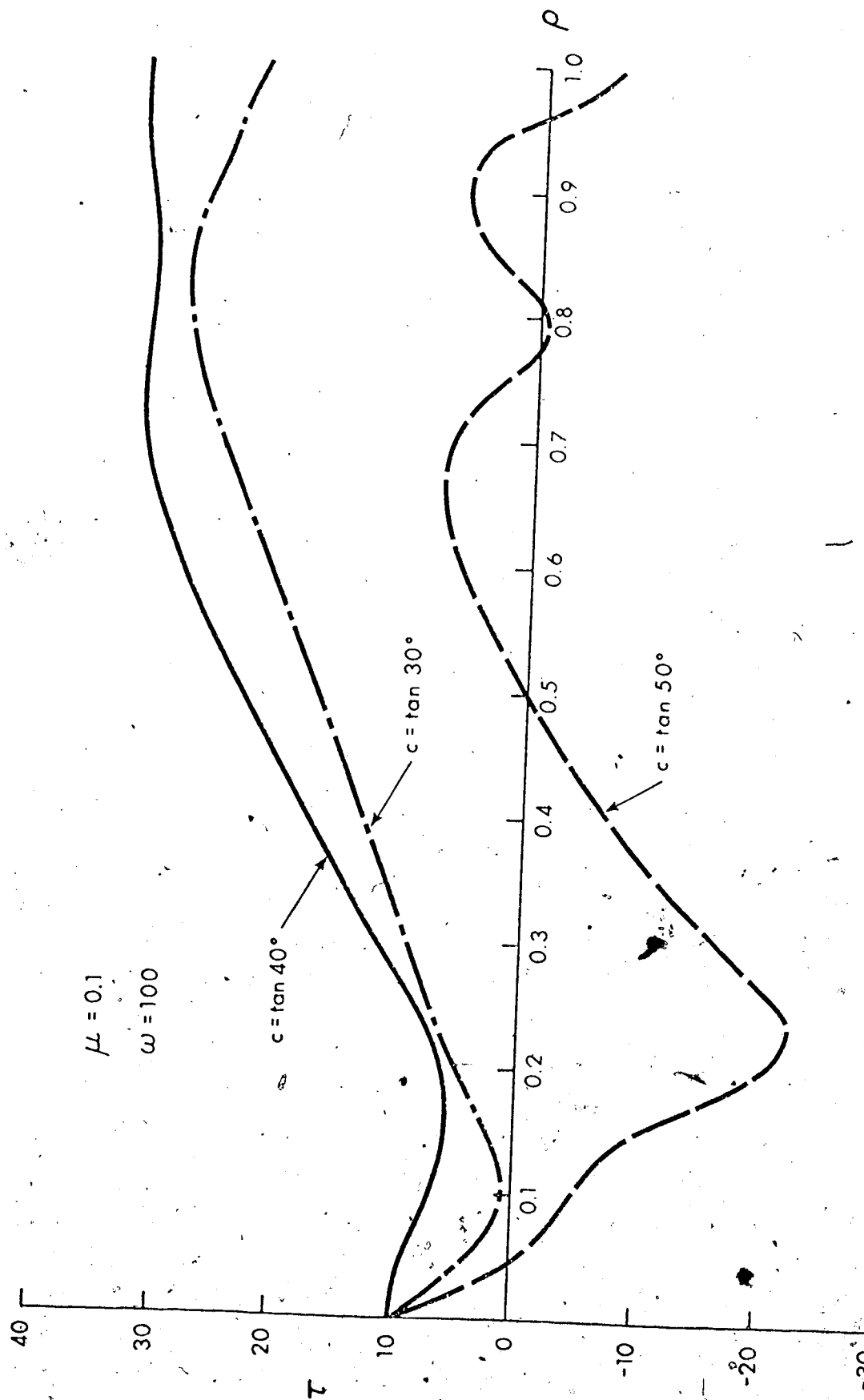


FIGURE 19: Nondimensional Tension for Polynomial Shapes

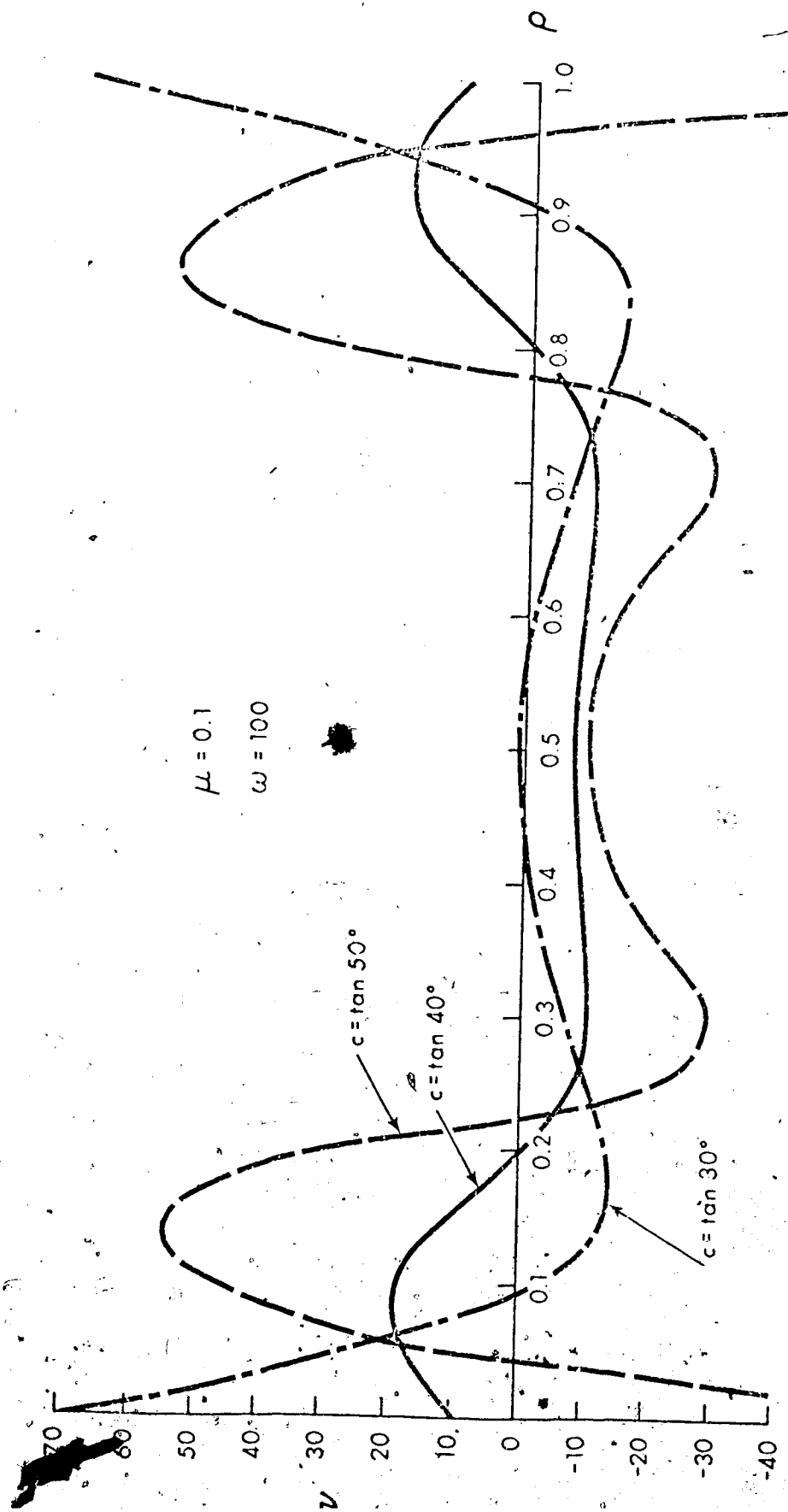


FIGURE 20: Nondimensional Shear Force for Polynomial Shapes

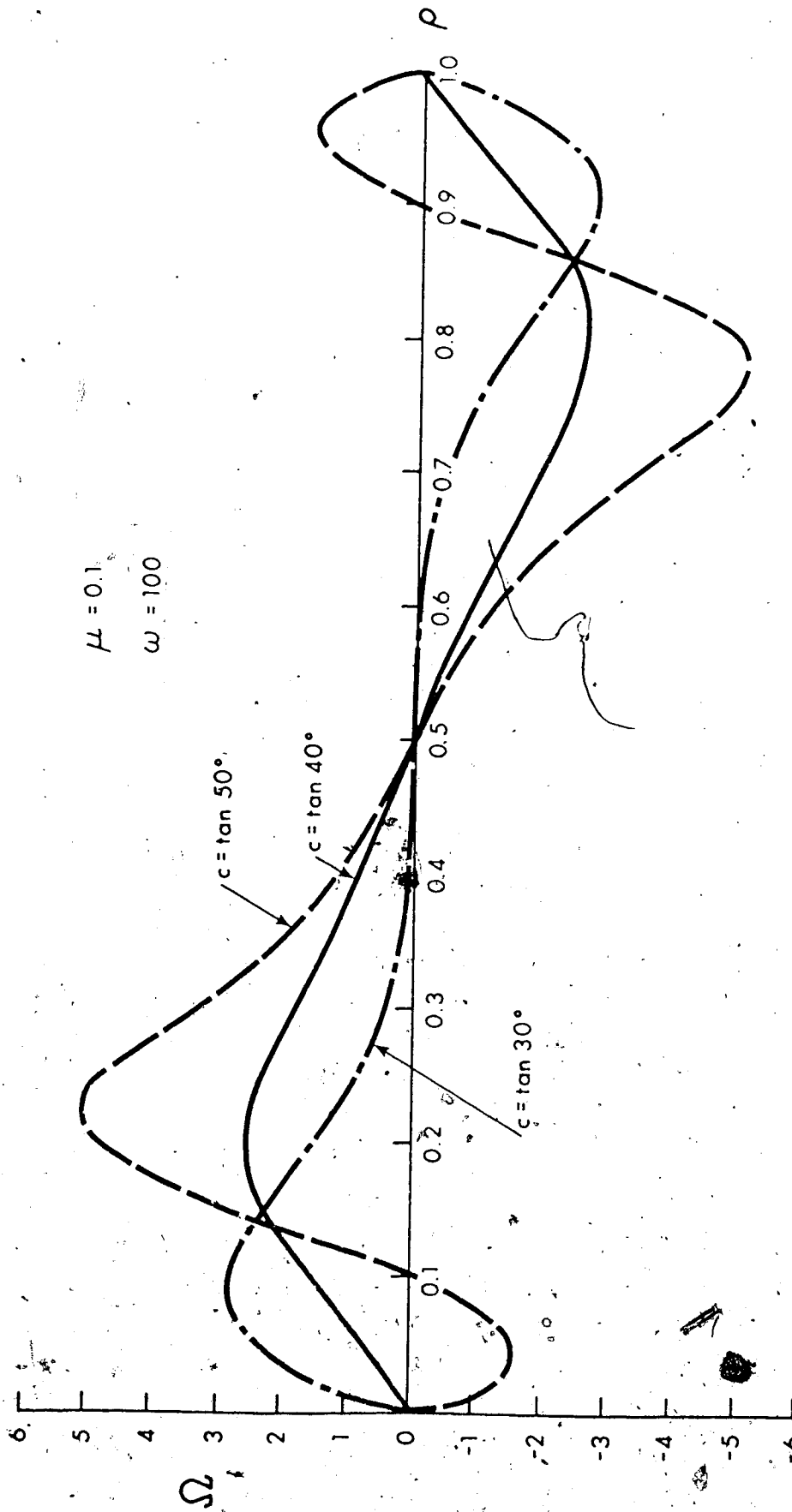


FIGURE 21: Nondimensional Moment for Polynomial Shapes

## CHAPTER V

## EXPERIMENTAL CONSIDERATIONS

5.1 Experimental Procedure

Experimental verification of the numerical solution for the stiffened catenary problem considered in section 3.5.3. is given in this chapter.

The boundary conditions for this problem can be duplicated experimentally. The procedure followed was to suspend a 6 foot long, 1/16 inch diameter steel rod by thin threads at both ends. A Cooke, Troughton and Simms precision level was used to position the ends of the rod at the same level. The coordinates of six points along one half the rod were measured using a cathetometer (made by Gaertner Scientific Corporation) and a 30 inch long brass scale clamped to the edge of a 2.5 foot by 5.0 foot surface table as shown in Figure 22. The cathetometer was used to measure the vertical coordinates of points along the rod. Its telescope and micrometer screw have a displacement of only 2 inches, thus larger displacements had to be measured in several increments. The horizontal coordinates of points along the rod were measured using the brass scale in conjunction with a vernier scale attached to the base of the cathetometer. These coordinates were measured for three different slopes of the supporting threads. These slopes were determined by measuring the horizontal and vertical distances between two points on the threads using the brass scale and cathetometer. The experimental data is given in Appendix II.

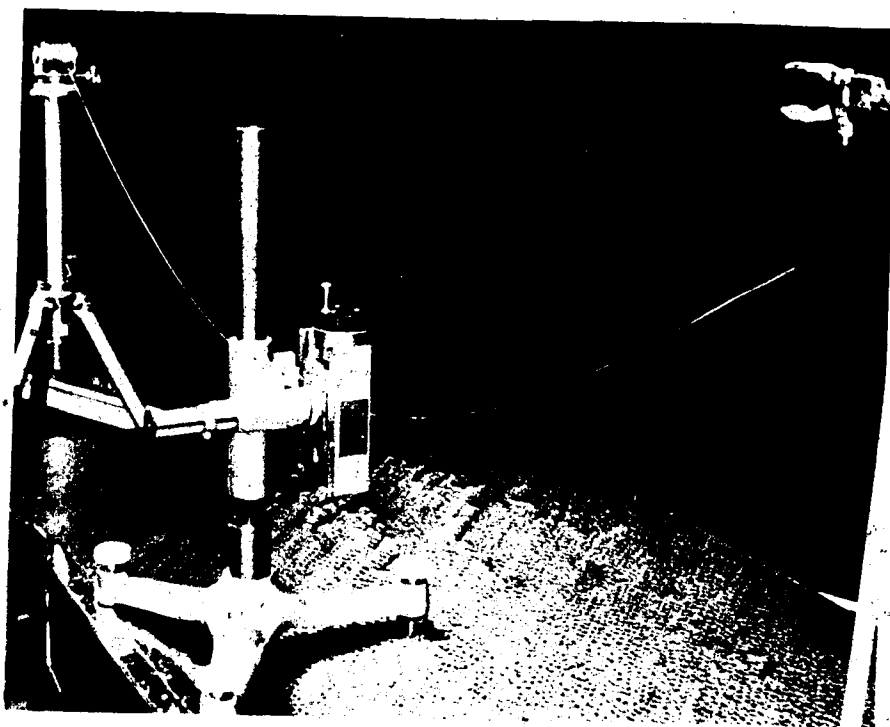


FIGURE 22: Experimental Apparatus

## 5.2 Calculations and Results

The nondimensional coordinates of the deformed rod are given by

$$\begin{aligned} X^* &= X/L \\ Y^* &= Y/L \end{aligned} \quad (5.1)$$

where  $X$ ,  $Y$  and  $L$  are shown in Figure 11. The values of these coordinates at points along the rod as calculated from the experimental data using equation (5.1) are shown in Figure 23.

The angle  $\alpha$  defined in Figure 11 is given by

$$\alpha = \arctan (\Delta_Y / \Delta_X) \quad (5.2)$$

where  $\Delta_X$  and  $\Delta_Y$  are the horizontal and vertical distances between two points on the supporting threads. The values of  $\alpha$  calculated from the experimental measurements of  $\Delta_Y$  and  $\Delta_X$  are given in Appendix III (Table 8).

The nondimensional weight of the rod as defined in section 3.5.3. is given by

$$W^* = \frac{64 (WL) L^2}{\pi D^4 E} \quad (5.3)$$

for a circular rod of diameter  $D$ . For the rod used in the experiment

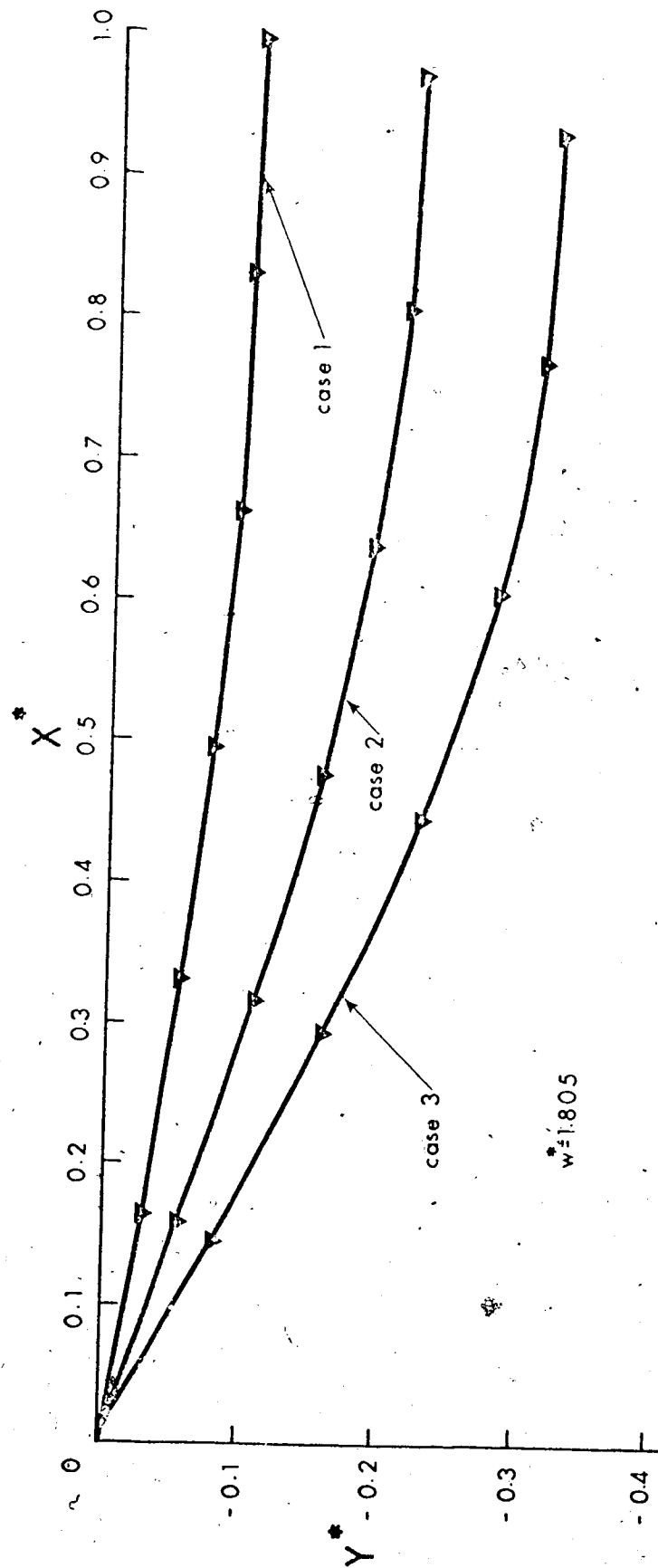


FIGURE 23: Experimental Stiffened Catenary Shapes



with  $E = 29.8 \times 10^6$  psi, the nondimensional weight is  $W^* = 1.805$ :

Using this value of  $W^*$  and the values of  $\alpha$  given in Table 8 the numerical solution for the shapes of the rod can be evaluated.

These shapes are compared to the experimentally determined points in Figure 23.

### 5.3 Error Analysis

The deformed shape of the rod has been determined experimentally by measuring the coordinates of points along the rod. It has also been found by experimentally determining the loading parameters for the rod and then using the numerical method to calculate the shape of the rod. Both solutions are based on experimentally measured quantities which have some error associated with them.

If  $x$  is the measured value of a quantity with correct value  $q$ , the error is defined as

$$e = |q - x| \quad (5.4)$$

If the quantity  $q$  is a function of several quantities, say  $q = F(a, b, c, d)$  then the error  $e(q)$  is given by

$$e^2(q) = \sum_{n=a}^d \left( \frac{\partial F}{\partial n} \right)^2 e^2(n) \quad (5.5)$$

when the errors  $e(a)$ ,  $e(b)$ ,  $e(c)$  and  $e(d)$  are symmetric and independent (see Reference [5]).

The largest differences between the experimentally determined coordinates and the values found using the numerical method occur at the lowest point of the catenary. The values of the X coordinates and vertical deflection at this point are  $h$  and  $d$  as shown in Figure 11.

The values of these quantities measured experimentally are referred to as  $h_E$  and  $d_E$ , and those calculated using the numerical method as  $h_N$  and  $d_N$ .

The nondimensional values of these quantities are

$$h^* = \frac{h}{L^2} \quad \text{and} \quad d^* = \frac{d}{L} \quad (5.6)$$

Using equations (5.5) and (5.6) the relative errors in  $h_E^*$  and  $d_E^*$  are given by

$$\epsilon^2(h_E^*) = \epsilon^2(h) + \epsilon^2(L) \quad (5.7)$$

$$\epsilon^2(d_E^*) = \epsilon^2(d) + \epsilon^2(L)$$

where the relative error of the quantity  $q$  is defined as

$$\epsilon(q) = \frac{e(q)}{q} \quad (5.8)$$

$\epsilon(h)$ ,  $\epsilon(d)$  and  $\epsilon(L)$  are the relative errors in the measured values  $h$ ,  $d$  and  $L$ .

Determining  $\epsilon(h_N^*)$  and  $\epsilon(d_N^*)$  is more complicated. The quantities  $h_N^*$  and  $d_N^*$  are functions of the quantities  $W^*$  and  $\alpha$  which in turn are functions of several experimentally measured quantities.

Using equations (5.3), (5.5) and (5.8) gives the relative error in the nondimensional weight as

$$\epsilon^2(W^*) = \epsilon^2(WL) + 4\epsilon^2(L) + \epsilon^2(E) + 16\epsilon^2(D) \quad (5.9)$$

Similarly the relative error in  $\alpha$  is given by

$$\epsilon(\alpha) = \pm \frac{[\Delta_X^2 e^2(\Delta_Y) + \Delta_Y^2 e^2(\Delta_X)]^{1/2}}{(\Delta_X^2 + \Delta_Y^2) \alpha} \quad (5.10)$$

After calculating  $\epsilon(\alpha)$  and  $\epsilon(W^*)$  the relative errors in  $h_N^*$  and  $d_N^*$  are given by

$$\begin{aligned} \epsilon^2(d_N^*) &= \left[ \frac{\alpha}{d_N^*} \frac{\partial d_N^*}{\partial \alpha} \right]^2 \epsilon^2(\alpha) + \left[ \frac{W^*}{d_N^*} \frac{\partial d_N^*}{\partial W^*} \right]^2 \epsilon^2(W^*) \\ \epsilon^2(h_N^*) &= \left[ \frac{\alpha}{h_N^*} \frac{\partial h_N^*}{\partial \alpha} \right]^2 \epsilon^2(\alpha) + \left[ \frac{W^*}{h_N^*} \frac{\partial h_N^*}{\partial W^*} \right]^2 \epsilon^2(W^*) \end{aligned} \quad (5.11)$$

The partial derivative must be evaluated numerically from the numerical solution. The values of  $h_N^*$ ,  $d_N^*$  and the partial derivatives calculated with the three values of  $\alpha$  and  $W^* = 1.805$  are given in Appendix III.

Using the data in Appendix I the relative errors  $\epsilon(h_E^*)$  and  $\epsilon(d_E^*)$  were calculated from equation (5.7). These are given in Table 5.

The relative errors  $\epsilon(W^*)$  and  $\epsilon(\alpha)$  were calculated from equations (5.9) and (5.10) from the experimental data with  $\epsilon(E) = \pm 1\%$ . The relative errors  $\epsilon(h_N^*)$  and  $\epsilon(d_N^*)$  were then calculated from equation (5.11) using the quantities in Appendix III. These relative errors expressed as a percentage are given in Table 5.

TABLE 5

Percentage Errors in the Numerical and Experimental Solutions

	Case 1	Case 2	Case 3
$\epsilon(d_E^*)$	$\pm 0.5$	$\pm 0.3$	$\pm 0.2$
$\epsilon(d_N^*)$	$\pm 0.6$	$\pm 1.4$	$\pm 1.6$
$\epsilon(h_E^*)$	$\pm 0.1$	$\pm 0.1$	$\pm 0.1$
$\epsilon(h_N^*)$	$\pm 0.01$	$\pm 0.1$	$\pm 0.2$

The differences between the numerical and experimental values of  $d^*$  and  $h^*$  were calculated. In all cases this difference was less than the sum of errors given by the two methods. That is

$$|d_E^* - d_N^*| < |e(d_E^*)| + |e(d_N^*)|$$

and

$$|h_E^* - h_N^*| < |e(h_E^*)| + |e(h_N^*)|$$

This means there is a region of intersection of the interval  $d_E^* \pm e(d_E^*)$  and the interval  $d_N^* \pm e(d_N^*)$  and similarly for  $h_N^*$  and  $h_E^*$ . It can be concluded that within the accuracy of this experiment no significant difference was found between the numerical solution and the experimental results.

## CHAPTER VI

## CONCLUDING REMARKS

6.1 Summary

The pipeline problem mentioned at the beginning of this thesis requires solution to two types of problems of nonlinear bending of thin rods. These have been considered for the case of an initially straight rod.

A general numerical method has been presented to solve the problem of determining the deformed shape of an initially straight rod when the loading is given. This method can be used to solve problems of rods with varying flexural stiffness and with any combination and number of concentrated forces, couples and nonuniform distributed loads applied to the rod. Because of the use of only one segment of the rod at a time in the numerical method, the calculations can be done on a small computing facility such as the HP9820A desk top programmable calculator.

The problem of finding the distributed loading necessary to deform a straight rod to a specified shape has also been considered. Normal and tangential distributed loads in combination with a uniform gravitational load were used. A general numerical integration technique was developed for problems where the specified shape is given in Cartesian coordinates. From the example problem considered

in section 4.5 it can be seen that small changes in the specified shape of the rod lead to large changes in the required distributed loads.

An experimental verification of the numerical method for the problem of the stiffened catenary has been given. The experimentally determined deformed shape and the numerical solution agree within the estimated experimental errors for the particular rod considered.

## 6.2 Areas of Further Research

The methods and solutions mentioned above can be extended to consider rods which are initially curved. For the problem of finding the required loading to bend a rod to a specified shape it is possible to consider the shape given in polar coordinates or through parametric equations. In the solution of this problem the function defining the shape of the rod must be differentiated several times. Also if the shape is specified as a set of discrete points then some interpolation function must be used to determine the required loading. These steps can be avoided by using a variation of the numerical method used to solve the problem of unknown deformed shape. If the rod is divided into a series of segments each loaded by a uniformly distributed or concentrated load then the values of these loads could be determined using a one dimensional secant method so that the rod passes through specified points of the required shape function. The segment solutions needed have already been developed for the problem of unknown deformed shape.

The dynamic problem of determining the natural frequencies and modes of vibration of the rods mentioned above could also be considered. This may be of some importance in the laying of offshore pipelines as they can be excited by ocean currents.



## BIBLIOGRAPHY

- [1] Barton, H.J., "On the Deflection of a Cantilever Beam", *Quarterly of Applied Mathematics*, Vol. 2, No. 2, July 1944, pp. 168-171; Vol. 3, No. 3, Oct. 1945, pp. 275-276 (correction).
- [2] Bickley, W.J., "The Heavy Elastica", *Philosophical Magazine*, 7th Series, Vol. 17, No. 113, March 1934, pp. 603-622.
- [3] Bisshopp, K.E. and Drucker, D.C., "Large Deflection of Cantilever Beams", *Quarterly of Applied Mathematics*, Vol. 3, No. 3, Oct. 1945, pp. 272-275.
- [4] Boyd, J.E., *Strength and Materials*, 3rd Edition, Appendix D, McGraw-Hill, New York, 1924.
- [5] Cook, N.H. and Rabinowicz, E., *Physical Measurement and Analysis*, Addison-Wesley Publishing Company, Reading, Mass., 1963.
- [6] Conway, H.D., "The Large Deflection of Simply Supported Beams", *Philosophical Magazine*, Vol. 38, No. 287, Dec. 1947, pp. 905-911.
- [7] Conway, H.D., "The Nonlinear Bending of Thin Circular Rods", *Journal of Applied Mechanics*, Vol. 23, March 1956, pp. 7-10.
- [8] Daley, G.C., "Optimization of Tension Level and Stinger Length for Offshore Pipeline Installation", *Journal of Engineering for Industry*, Vol. 96, No. 4, 1974, pp. 1334-1336.
- [9] Frisch-Fay, R., *Flexible Bars*, Butterworths, London, 1962.
- [10] Garlicki, A.M. and Mirza, S., "The Mechanics of Band Saw Blades", *Symposium on Applications of Solid Mechanics*, University of Waterloo, 1972, pp. 193-222.

- [11] Gospodnetic, D., "Deflection Curve of a Simply Supported Beam",  
Journal of Applied Mechanics, Vol. 26, Dec. 1959, pp. 675-  
676.
- [12] Gross, S. and Lehr, E., Die Federn, V.D.I. - Verlag, Berlin, 1938.
- [13] Holden, J.T., "On the Finite Deflection of Thin Beams", Inter-  
national Journal of Solids and Structures, Vol. 8, No. 8,  
Aug. 1972, pp. 1051-1055.
- [14] Hummel, F.H. and Morton, W.B., "On the Large Bending of Thin  
Flexible Strips and the Measurement of Their Elasticity",  
Philosophical Magazine, 7th Series, Vol. 4, No. 21, Aug.  
1927, pp. 348-357.
- [15] Iyengar, S.R. and Rao, S.K.L., "Large Deflections of Simply  
Supported Beams", Journal of The Franklin Institute, Vol.  
259, No. 6, June 1955, pp. 523-528.
- [16] Lippmann, H., Mahrenholtz, O. and Johnson, W., "Thin Heavy Elastic  
Strips at Large Deflexions", International Journal of  
Mechanical Sciences, Vol. 2, No. 4, 1961, pp. 294-310.
- [17] Mitchell, T.P., "The Nonlinear Bending of Thin Rods", Journal  
of Applied Mechanics, Vol. 26, March 1959, pp. 40-43.
- [18] Rohde, F.V., "Large Deflections of a Cantilever Beam with a  
Uniformly Distributed Load", Quarterly of Applied Mathematics,  
Vol. 11, No. 3, Oct. 1953, pp. 337-338.
- [19] Saelman, B., "Some Formulas for Large Deflections of Beam Columns",  
Journal of The Franklin Institute, Vol. 257, No. 2, Feb. 1954,  
pp. 125-132.

- [20] Sato, K., "Large Deflection of Thin Circular Cantilever Beams",  
Journal of Applied Mechanics, Vol. 25, June 1958, pp. 294-  
295.
- [21] Schmidt, R., and DaDeppo, D.A., "Large Deflections of Heavy  
Cantilever Beams and Columns", Quarterly of Applied  
Mathematics, Vol. 28, No. 3, Oct. 1970, pp. 441-444.
- [22] Seames, A.E. and Conway, J., "A Numerical Procedure for Calculating  
the Large Deflections of Straight and Curved Beams", Journal  
of Applied Mechanics, Vol. 24, No. 2, June, 1957, pp. 289-  
294.
- [23] Spenceley, G.W. and Spenceley, R.M., Smithsonian Elliptic Function  
Tables, The Smithsonian Institute, Washington, 1947.
- [24] Tada, Y. and Lee, G.C., "Finite Element Solution to an Elastica  
Problem of Beams", International Journal for Numerical  
Methods in Engineering, Vol. 2, No. 2, 1970, pp. 229-241.
- [25] Timoshenko, S.P., History of Strength and Materials, McGraw-Hill,  
New York, 1953.
- [26] Truesdell, C., "A New Chapter in the Theory of the Elastica",  
Proceedings of the First Midwestern Conference of Solid  
Mechanics, 1953, pp. 52-54.
- [27] Verma, M.K. and Krishna Murty, A.V., "Nonlinear Bending of Beams  
of Variable Cross Section", International Journal of  
Mechanical Sciences, Vol. 15, No. 2, Feb. 1973, pp. 183-187.

- [28] Wang, T.M., "Nonlinear Bending of Beams with Concentrated Loads",  
Journal of The Franklin Institute, Vol. 285, No. 5, May, 1968,  
pp. 386-390.
- [29] Wang, T.M., Lee, S.L. and Zienkiewicz, O.C., "A Numerical Analysis  
of Large Deflections of Beams", International Journal of  
Mechanical Sciences, Vol. 3, No. 3, 1961, pp. 219-228.
- [30] Yang, T.Y., "Matrix Displacement Solution to Elastica Problems of  
Beams and Frames", International Journal of Solids and  
Structures, Vol. 9, No. 7, 1973, pp. 829-842.

## APPENDIX I

## GENERAL PROGRAM FOR THE NUMERICAL METHOD OF CHAPTER III

This program has been set up to solve the boundary value problem as in section 3.4. It can be used to solve problems with varying distributed loads and nonuniform cross sections by considering the rod as a series of segments with uniform cross sections and uniform distributed loads which approximate the distributed loading and rod cross sections.

The first part of the program solves the initial value problem as described in section 3.4.1. This can be used with loads  $\chi$  and  $\psi$  in the segment or with tangential loads  $\xi$  and  $\eta$ . The second part of the program is used to find the unknown initial conditions in the boundary value problem. It has been written for the case of one and two unknown initial conditions. The case for three unknown quantities can be set up using the equations in section 3.4.2.

The program has been written with the form of language used in the 9820A Hewlett Packard programmable desk computer. The register numbers (R1, R2, ... etc) used in the actual program have been replaced by the variable names. The arrow used in the program statements indicates that the expression to the left of the arrow is calculated and assigned to the register representing the quantity to the right of the arrow. In the first part of the program the

subscript  $j$  which was used in section 3.3 and section 3.4 to indicate the  $j^{\text{th}}$  segment has been dropped. Line 5 and 6 are used to assign known and unknown initial conditions at the beginning of the rod for a particular boundary value problem. Line 7 assigns the value of the ratio of segment flexural rigidity to the reference rigidity as defined in equation (3.18). Line 10 assigns values to the constant segment distributed loads  $\chi_j$  and  $\psi_j$  or  $\eta_j$  and  $\xi_j$ . Line 21 is used to terminate the element series solution.

For one unknown initial condition the one dimensional form of equation (3.36) given by equation (3.42) must be solved for  $Z$  which is assigned to the unknown initial condition in line 5 or 6. The quantity  $q^*$  is the specified value of the quantity  $q$  which is given at the end of the rod. One of the quantities  $B^*$ ,  $D^*$ ,  $G^*$ ,  $X^*$ ,  $Y^*$ ,  $\gamma$  at the end of the rod is assigned to  $q$  in line 34 of the General Program Part 2 (with 1-D Secant). The one dimensional form of the iteration given by equations (3.37) and (3.38) is

$$Z^{i+1} = Z^i - \frac{(Z^i - Z^{i-1}) p(Z^i)}{p(Z^i) - p(Z^{i-1})}$$

Two initial guesses  $Z^0$  and  $Z^1$  must be used to start this iteration.

With two unknown initial conditions the General Program Part 2 (with 2-D Secant Method) must be used to solve the equations

$$p_1(Z_1, Z_2) = q_1(Z_1, Z_2) - q_1^* = 0$$

$$p_2(z_1, z_2) = q_2(z_1, z_2) - q_2^* = 0$$

where  $z_1, z_2$  are the unknown initial conditions at the start of the rod assigned in lines 5 and 6 and  $q_1^*$  and  $q_2^*$  are the required values of  $q_1$  and  $q_2$  which are the quantities specified at the end of the rod and assigned in lines 34.

The iteration used in this program is the two dimensional form of that given by equations (3.37) and (3.38).

$$z_1^{(i+1)} = z_1^i - [J_{22} p_1(z_1^i, z_2^i) - J_{12} p_2(z_1^i, z_2^i)]/D$$

$$z_2^{(i+1)} = z_2^i - [J_{11} p_2(z_1^i, z_2^i) - J_{21} p_1(z_1^i, z_2^i)]/D$$

where

$$J_{11} = [p_1(z_1^i, z_2^i) - p_1(z_1^{i-1}, z_2^i)]/(z_1^i - z_1^{i-1})$$

$$J_{12} = [p_1(z_1^i, z_2^i) - p_1(z_1^i, z_2^{i-1})]/(z_2^i - z_2^{i-1})$$

$$J_{21} = [p_2(z_1^i, z_2^i) - p_2(z_1^{i-1}, z_2^i)]/(z_1^i - z_1^{i-1})$$

$$J_{22} = [p_2(z_1^i, z_2^i) - p_2(z_1^i, z_2^{i-1})]/(z_2^i - z_2^{i-1})$$

$$D = J_{11} J_{22} - J_{21} J_{12}$$

Initial guesses  $(Z_1^0, Z_2^0)$  and  $(Z_1^1, Z_2^1)$  must be used to start this iteration.

General Program - Part 1 (with distributed segment loads  $\chi_j$  and  $\psi_j$ )

$N$  = number of segments used.  $N_p$  = number of points at which data is printed.

1. Enter,  $N, N_p$ , [loading parameters for a particular problem].
2. Print,  $N, N_p$ , [loading parameters for a particular problem].
3. GOTO 37.
4.  $1 \rightarrow J$ .
5. [ ]  $\rightarrow X^*$ ; [ ]  $\rightarrow Y^*$ ; [ ]  $\rightarrow \gamma$ .
6. [ ]  $\rightarrow A^*$  [ ]  $\rightarrow C^*$  [ ]  $\rightarrow F^*$ .
7. [ ]  $\rightarrow r$ .
8.  $A^*/(rN) \rightarrow a$ ;  $C^*/(rN^2) \rightarrow c$ ;  $F^*/(rN^2) \rightarrow f$ .
9.  $-(3a + f)/6 \rightarrow \beta$ .
10. [ ]  $\rightarrow \chi$ ; [ ]  $\rightarrow \psi$ .
11.  $4 \rightarrow k$ .
12.  $\beta \rightarrow \alpha_{k-4}$ ;  $a \rightarrow \alpha_{k-3}$ ;  $f/2 \rightarrow \alpha_{k-2}$ ;  $(ca - \chi\beta - \psi)/6 \rightarrow \alpha_{k-1}$ .
13.  $\alpha_{k-4} + \alpha_{k-3} + \alpha_{k-2} + \alpha_{k-1} \rightarrow \phi$ .
14.  $\alpha_{k-3} + 2\alpha_{k-2} + 3\alpha_{k-1} \rightarrow b$ .
15.  $2\alpha_{k-2} + 6\alpha_{k-1} \rightarrow g$ .



16.  $\alpha_{k-4} + \alpha_{k-3}/2 + \alpha_{k-2}/3 + \alpha_{k-1}/4 \rightarrow h.$
17.  $(c\alpha_{k-2} - \chi\alpha_{k-3})/(k(k-1)) \rightarrow \alpha_k.$
18.  $\phi + \alpha_k \rightarrow \phi; b + k\alpha_k \rightarrow b.$
19.  $g + k(k-1)\alpha_k \rightarrow g; h + \alpha_k/(k+1) \rightarrow h.$
20.  $\alpha_{k-2} \rightarrow \alpha_{k-3}; \alpha_{k-1} \rightarrow \alpha_{k-2}; \alpha_k \rightarrow \alpha_{k-1}; k+1 \rightarrow k.$
21. If  $ABS[\alpha_k + \alpha_{k-1} + \alpha_{k-2}] > [ ]$ ; GOTO 17.
22.  $c + f\beta - g\phi - \chi \rightarrow d.$
23.  $X^* + (\cos(\gamma-\beta) - h\sin(\gamma-\beta))/N \rightarrow X^*.$
24.  $Y^* + (\sin(\gamma-\beta) + h\cos(\gamma-\beta))/N \rightarrow Y^*.$
25.  $\gamma - \beta + \phi \rightarrow \gamma.$
26.  $brN \rightarrow B^*; drN^2 \rightarrow D^*; grN^2 \rightarrow G^*.$
27. If  $Q \neq 1$ ; GOTO 31.
28. If  $ABS \sin(J\pi N_p/N) > 1E-6$ ; GOTO 31.
29. PRINT, J, B\*, D\*, G\*.
30. PRINT, X\*, Y\*,  $\gamma$ .
31.  $B^* \rightarrow A^*; D^* \rightarrow C^*; G^* \rightarrow F^*.$
32. If  $J \neq N$ ;  $J+1 \rightarrow J$ ; GOTO 7.
33. If  $Q = 1$ ; GOTO [END].

General Program - Part 1 (with distributed segment normal and tangential

loads  $\eta_j$  and  $\xi_i$ )

Modifications to General Program - Part 1 (with loads  $\chi_j$  and  $\psi_j$ ).

10.  $[ ] \rightarrow \xi; [ ] \rightarrow \eta.$
12.  $\beta \rightarrow \alpha_{k-4}; a \rightarrow \alpha_{k-3}; f/2 \rightarrow \alpha_{k-2}; (ca-\eta)/6 \rightarrow \alpha_{k-1}.$

$$17. (c\alpha_{k-2} - \xi \alpha_{k-3}(1+1/k))/(k(k-1)) \rightarrow \alpha_k.$$

$$22. c + f\beta - g\phi - \xi - \eta h \rightarrow d.$$

General Program - Part 2 (1-D Secant Method)

34. [ ]  $\rightarrow$  q.
35. If R = 1; GOTO 41.
36. If R = 2; GOTO 43.
37. ENTER  $Z^0, Z^1, q^*$ .
38. PRINT  $Z^0, Z^1, q^*$ .
39.  $Z^0 \rightarrow Z^{i-1}; Z^1 \rightarrow Z^i$ .
40.  $Z^{i-1} \rightarrow Z; 1 \rightarrow R$ ; GOTO 4.
41.  $q - q^* \rightarrow p^{i-1}$ .
42.  $Z^i \rightarrow Z; 2 \rightarrow R$ ; GOTO 4.
43.  $q - q^* \rightarrow p^i$ ; PRINT, i,  $p^i, Z^i$ .
44. If ABS  $p^i < [ ]$ ;  $1 \rightarrow Q$ ; GOTO 4.
45.  $Z^i - ((Z^i - Z^{i-1})/(p^i - p^{i-1})) p^i \rightarrow Z^{i+1}$ .
46.  $Z^i \rightarrow Z^{i-1}; p^i \rightarrow p^{i-1}$ .
47.  $Z^{i+1} \rightarrow Z^i$ .
48.  $1 + i \rightarrow i$ ; GOTO 42.
49. END.

General Program - Part 2 with Two-Dimensional Secant Method

34. [ ]  $\rightarrow q_1$ ; [ ]  $\rightarrow q_2$ .
35. If R = 1; GOTO 44.

36. If  $R = 2$ ; GOTO 48.
37. If  $R = 3$ ; GOTO 50.
38. ENTER,  $Z_1^0, Z_2^0, Z_1^1, Z_2^1, q_1^*, q_2^*$ .
39. PRINT,  $Z_1^0, Z_2^0, Z_1^1, Z_2^1, q_1^*, q_2^*$ .
40.  $1 \rightarrow i; 0 \rightarrow Q$ .
41.  $Z_1^0 \rightarrow Z_1^{i-1}; Z_2^0 \rightarrow Z_2^{i-1}$ .
42.  $Z_1^1 \rightarrow Z_1^i; Z_2^1 \rightarrow Z_2^i$ .
43.  $Z_1^i \rightarrow Z_1; Z_2^i \rightarrow Z_2; 1 \rightarrow R$ ; GOTO 4.
44.  $q_1 - q_1^* \rightarrow p_1(i, i); q_2 - q_2^* \rightarrow p_2(i, i)$ .
45. PRINT,  $i, p_1^i, p_2^i, Z_1^i, Z_2^i$ .
46. If  $ABS[p_1^i] < [ ]$  and  $ABS[p_2^i] < [ ]$ ;  $1 \rightarrow Q$ ; GOTO 4.
47.  $Z_1^i \rightarrow Z_1; Z_2^{i-1} \rightarrow Z_2; 2 \rightarrow R$ ; GOTO 4.
48.  $q_1 - q_1^* \rightarrow p_1(i, i-1); q_2 - q_2^* \rightarrow p_2(i, i-1)$ .
49.  $Z_1^{i-1} \rightarrow Z_1; Z_2^{i-1} \rightarrow Z_2; 3 \rightarrow R$ ; GOTO 4.
50.  $q_1 - q_1^* \rightarrow p_1(i-1, i); q_2 - q_2^* \rightarrow p_2(i-1, i)$ .
51.  $[p_1(i, i) - p_1(i-1, i)] / (Z_1^i - Z_1^{i-1}) \rightarrow J_{11}$ .
52.  $[p_1(i, i) - p_1(i, i-1)] / (Z_2^i - Z_2^{i-1}) \rightarrow J_{12}$ .
53.  $[p_2(i, i) - p_2(i-1, i)] / (Z_1^i - Z_1^{i-1}) \rightarrow J_{21}$ .
54.  $[p_2(i, i) - p_2(i, i-1)] / (Z_2^i - Z_2^{i-1}) \rightarrow J_{22}$ .
55.  $J_{11} J_{22} - J_{21} J_{12} \rightarrow D$ .
56.  $Z_1^i - [J_{22} p_1(i, i) - J_{12} p_2(i, i)] / D \rightarrow Z_1^{i+1}$ .
57.  $Z_2^i - [J_{11} p_2(i, i) - J_{21} p_1(i, i)] / D \rightarrow Z_2^{i+1}$ .
58.  $Z_1^i \rightarrow Z_1^{i-1}; Z_2^i \rightarrow Z_2^{i-1}$ .
59.  $Z_1^{i+1} \rightarrow Z_1^i; Z_2^{i+1} \rightarrow Z_2^i$ .

60.  $i + 1 \rightarrow i$ ; GOTO 43.

61. END.

### Specialized Lines to Solve Particular Boundary Value Problems

Some lines of the general program must be specialized for solving a particular problem. These lines are shown below for the problems treated in section 3.5.

#### Elastica Problem

General Program - Part 1 (with distributed loads  $\chi_j$  and  $\psi_j$ ).

1. ENTER N,  $N_p$ ,  $P^*$ .
2. PRINT N,  $N_p$ ,  $P^*$ .
5.  $0 \rightarrow X^*$ ;  $0 \rightarrow Y^*$ ;  $Z \rightarrow \gamma$ .
6.  $0 \rightarrow A^*$ ;  $-P^* \cos \gamma \rightarrow C^*$ ;  $-P^* \sin \alpha \rightarrow F^*$ .
7.  $1 \rightarrow r$ .
10.  $0 \rightarrow \chi$ ;  $0 \rightarrow \psi$ .

General Program - Part 2 (with 1-D, secant method).

34.  $\gamma \rightarrow q$ .

Cantilever with Uniform Normal Load

General Program - Part 1 (with distributed loads  $\xi_j$  and  $\eta_j$ ).

1. ENTER N,  $N_p$ , P\*.
2. PRINT W,  $N_p$ , P\*.
5.  $0 \rightarrow X^*$ ;  $0 \rightarrow Y^*$ ;  $Z \rightarrow \gamma$ .
6.  $0 \rightarrow A^*$ ;  $0 \rightarrow C^*$ ;  $0 \rightarrow F^*$ .
7.  $1 \rightarrow r$ .
10.  $0 \rightarrow \xi$ ;  $P^*/(rN^3) \rightarrow \eta$ .

General Program - Part 2 (with 1-D secant method).

34.  $\gamma \rightarrow q$ .

Stiffened Catenary

General Program - Part 1 (with distributed loads  $\chi_j$  and  $\psi_j$ ).

1. ENTER N,  $N_p$ ,  $\alpha$ , W\*.
2. PRINT N,  $N_p$ ,  $\alpha$ , W\*.
5.  $0 \rightarrow X^*$ ;  $0 \rightarrow Y^*$ ;  $Z \rightarrow \gamma$ .
6.  $0 \rightarrow A^*$ ;  $W*(\text{ctn}\alpha \cos\gamma - \sin\gamma) \rightarrow C^*$ ;  $W*(\cos\alpha + \text{ctn}\alpha \sin\gamma) \rightarrow F^*$ .
7.  $1 \rightarrow r$ .
10.  $-W* \sin(\gamma-\beta)/(rN^3) \rightarrow \chi$ ;  $W* \cos(\gamma-\beta)/(rN^3) \rightarrow \psi$ .

General Program - Part 2 (with 1-D Secant).

34.  $\gamma \rightarrow q$ .

Nonuniform Cantilever (with specified distributed load and concentrated end load).

General Program - Part 1 (with distributed loads  $\chi_j$  and  $\psi_j$ ).

1. ENTER  $N, N_p, W_L^*, P^*, \alpha, t$ .
2. PRINT  $N, N_p, W_L^*, P^*, \alpha, t$ .
5.  $0 \rightarrow X^*; 0 \rightarrow Y^*; Z \rightarrow \gamma$ .
6.  $0 \rightarrow A^*; P^* \cos \alpha \rightarrow C^*; -P^* \sin \alpha \rightarrow F^*$ .
7.  $t + (J-.5)(1-t)/N \rightarrow r$ .
10.  $-W_L^* \sin(\gamma-\beta)/N^3 \rightarrow \chi; W_L^* \cos(\gamma-\beta)/N^3 \rightarrow \psi$

General Program - Part 2 (with 1-D Secant).

34.  $\gamma \rightarrow q$ .

Nonuniform Cantilever (with  $\gamma_0$  specified and no concentrated end load).

General Program - Part 1 (with distributed loads  $\chi_j$  and  $\psi_j$ ).

1. ENTER  $N, N_p, \gamma_0, t$ .
2. PRINT  $W, N_p, \gamma_0, t$ .
5.  $0 \rightarrow X^*; 0 \rightarrow Y^*; \gamma_0 \rightarrow \gamma$ .
6.  $0 \rightarrow A^*; 0 \rightarrow C^*; 0 \rightarrow F^*$ .

$$7. \quad t + (J-.5)(1-t)/N \rightarrow r.$$

$$10. \quad -Z \sin(\gamma-\beta)/N^3 \rightarrow \chi; Z \cos(\gamma-\beta)/N^3 \rightarrow \psi.$$

General Program - Part 2 (with 1-D secant).

$$34. \quad \gamma \rightarrow q.$$

## APPENDIX II

## EXPERIMENTAL DATA

The rod used in the experiment is composed of two 1/16 inch diameter welding rods welded together at the mid point of the rod.

Data for this rod is given below:

weight of half rod  $W_L = 28.2 \pm 0.1$  grams

length of half rod  $L = 36.0 \pm 0.03$  inches

diameter of rod  $D = 0.0625 \pm 0.0002$  inches.

To determine the slope of the threads supporting the rod the horizontal and vertical distance  $\Delta_X$  and  $\Delta_Y$  between two points on the thread were measured. These distances are given in Table 6.

The coordinates of the deformed shape of the rod measured for the slopes of the threads given by Table 6 are shown in Table 7.

TABLE 6

Horizontal and Vertical Distances Between Points on Thread

Case	$\Delta_X (\pm 0.02 \text{ in.})$	$\Delta_Y (\pm 0.002 \text{ in.})$
1	3.66	1.040
2	1.55	1.900
3	0.00	1.241



TABLE 7

Measured Coordinates of the Deflected Stiffened Catenary

$s$ (in.)	Case 1		Case 2		Case 3	
	$X(\pm .02 \text{ in.})$	$Y(\pm .02 \text{ in.})$	$X(\pm .02 \text{ in.})$	$Y(\pm .02 \text{ in.})$	$X(\pm .02 \text{ in.})$	$Y(\pm .02 \text{ in.})$
0	0.00	0.000	0.00	0.000	0.00	0.000
6	5.89	-0.971	5.63	-2.060	5.19	-2.957
12	11.84	-1.881	11.31	-3.997	10.50	-5.769
18	17.75	-2.677	17.02	-5.668	15.93	-8.195
24	23.74	-3.259	22.91	-6.931	21.66	-10.063
30	29.73	-3.575	28.85	-7.674	27.53	-11.194
36	35.74	-3.680	34.85	-7.930	33.53	-11.590

## APPENDIX III

## NUMERICAL SOLUTION

The values given in Table 8 were calculated using the numerical method to solve the stiffened catenary problem of section 3.5.3. This solution is compared to an experimental solution in Chapter V.

TABLE 8  
Quantities Calculated using the Numerical  
Solution for the Stiffened Catenary Problem  
with  $W^* = 1.805$

	Case 1	Case 2	Case 3
$\alpha$	0.2769	0.8805	1.571
$d^*$	0.1033	0.2219	0.3259
$\frac{\partial d^*}{\partial W^*}$	0.015	0.069	0.14
$\frac{\partial d^*}{\partial \alpha}$	0.28	0.15	0.18
$h^*$	0.9932	0.9687	0.9313
$\frac{\partial h^*}{\partial W^*}$	-0.0020	-0.020	-0.060
$\frac{\partial h^*}{\partial \alpha}$	-0.035	-0.043	-0.076